

A MICROWAVE SPECTROSCOPIC TECHNIQUE IN THE MEASURE OF
POLLUTANT SULFUR DIOXIDE IN THE ATMOSPHERE

by

Jeffrey Allen Beren

A Thesis Submitted to the Faculty of the
DEPARTMENT OF ELECTRICAL ENGINEERING
In Partial Fulfillment of the Requirements
For the Degree of
MASTER OF SCIENCE
In the Graduate College
THE UNIVERSITY OF ARIZONA

1 9 7 2

STATEMENT BY AUTHOR

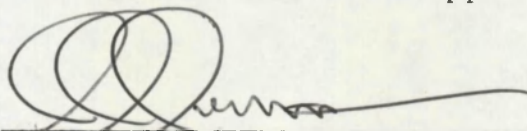
This thesis has been submitted in partial fulfillment of requirements for an advanced degree at The University of Arizona and is deposited in the University Library to be made available to borrowers under rules of the Library.

Brief quotations from this thesis are allowable without special permission, provided that accurate acknowledgment of source is made. Requests for permission for extended quotation from or reproduction of this manuscript in whole or in part may be granted by the head of the major department or the Dean of the Graduate College when in his judgment the proposed use of the material is in the interests of scholarship. In all other instances, however, permission must be obtained from the author.

SIGNED: Jeffrey Allen Beren

APPROVAL BY THESIS DIRECTOR

This thesis has been approved on the date shown below:



DONALD G. DUDLEY

Associate Professor of Electrical
Engineering

11/23/71
Date

ACKNOWLEDGMENTS

The author wishes to express his appreciation to Dr. Donald G. Dudley for his suggestion of the original problem and for his continued interest and guidance during this study.

The author would also like to thank his wife for her assistance in preparing the manuscript and Mr. and Mrs. W. H. Clark for the typing and final preparation of the manuscript.

TABLE OF CONTENTS

	Page
LIST OF ILLUSTRATIONS	v
LIST OF TABLES	vii
ABSTRACT	viii
INTRODUCTION	1
THEORY OF THE MICROWAVE ABSORPTION COEFFICIENT FOR ROTATIONAL ENERGIES OF GAS MOLECULES	5
Classical Theory of Molecular Energy and Absorption	5
Quantum Theory of Molecular Energy	9
Classification of Gas Molecules	15
Quantum Theory of Molecular Energy Applied to Classified Molecules	21
Quantum Theory of Molecular Absorption	25
APPLICATION OF THEORY TO ANALYSIS OF MEASUREMENT FEASIBILITY	34
Evaluation of Specific Constants of Equation (70) for Use with Sulfur Dioxide	34
Effect of Pressure Broadening Parameter	35
Cavity Frequency Meter Technique as Applied to Individual Lines	37
Cavity Frequency Meter Technique as Applied to Groups of Pressure Broadened Lines	43
EXPERIMENT CONCERNING FEASIBILITY OF MEASURING SULFUR DIOXIDE	54
CONCLUSION CONCERNING RECOMMENDATIONS FOR FUTURE STUDY IN THE INFRARED REGION	66
LIST OF SYMBOLS	73
SELECTED BIBLIOGRAPHY	74

LIST OF ILLUSTRATIONS

Figure	Page
1. Absorption Spectrum	2
2. Signal at Receiver	4
3. Dumbbell Rotor Model of a Diatomic Molecule	6
4. Dumbbell Rotor and Equivalent Particle	11
5. Dumbbell Rotor, Equivalent Particle Positions	12
6. Spectrum of a Diatomic Molecule	16
7. First Octant of the Ellipsoid	19
8. Inertia Ellipsoid of a Diatomic Molecule	20
9. Symmetric, Asymmetric Energy Level	24
10. Computer Listing	38
11. Sulfur Dioxide--Pure Concentration	39
12. Sulfur Dioxide--Single Line	40
13. Sulfur Dioxide--.01 ppm	42
14. Sulfur Dioxide--Line Width 1 GHz	44
15. Sulfur Dioxide--Line Width 3 GHz	45
16. Sulfur Dioxide--Line Width 11 GHz	46
17. Sulfur Dioxide--Line Width 19 GHz	47
18. Sulfur Dioxide--Concentration 1 ppm	49
19. Sulfur Dioxide--Concentration 10 ppm	50
20. Spectrum of H ₂ O and O ₂	52

LIST OF ILLUSTRATIONS--Continued

Figure	Page
21. Transmitter-Receiver System	56
22. Receiver System--Block Diagram	58
23. Transmitter Block Diagram	59
24. Link Map	60
25. Atmospheric Spectrum	61
26. Middle Infrared Spectrum	69
27. 8.6 μ Spectrum of SO ₂	71

LIST OF TABLES

Table	Page
1. Summary of Transmitter-Receiver System Specifications	62

ABSTRACT

The feasibility of using a microwave spectroscopic technique in the measure of a pollutant gas, sulfur dioxide, is discussed. In this technique the absorption spectrum of sulfur dioxide in the atmosphere is studied by remote microwave sensing.

The results of the study indicate that it is not at present feasible to measure sulfur dioxide in the microwave region because of the low resolution of the lines caused by the pressure broadening effect at atmospheric pressure. The technique of measuring the absorption spectrum seems applicable, however, in the infrared region and applied research should be conducted in this region.

INTRODUCTION

It has been demonstrated experimentally (Cleeton and Williams, 1934) that gas molecules with permanent dipole moments can absorb microwave radiation at certain discrete frequencies. The energy of this radiation is coupled into the molecule through the dipole moment and is stored as rotational energy in the molecule. Because of this property, it was the objective of this thesis to investigate the feasibility of measuring the absorption spectrum of a pollutant gas, sulfur dioxide, in the atmosphere. The basic idea was to transmit microwave radiation between two points and to record the amplitude of the received radiation as a function of frequency. At certain frequencies, a maximum amount of microwave radiation should be coupled into the pollutant gas and this should appear at the receiving point as a dip in the received amplitude at that certain frequency. By comparing the amplitude of the dip with the received amplitude at other frequencies, an indication of the amount of the pollutant gas present could be determined. In addition, variation of the dip at the same frequency would indicate a change in the level of concentration of the pollutant gas.

Figure 1 shows a plot of amplitude versus frequency for a fixed concentration and fixed line width for a

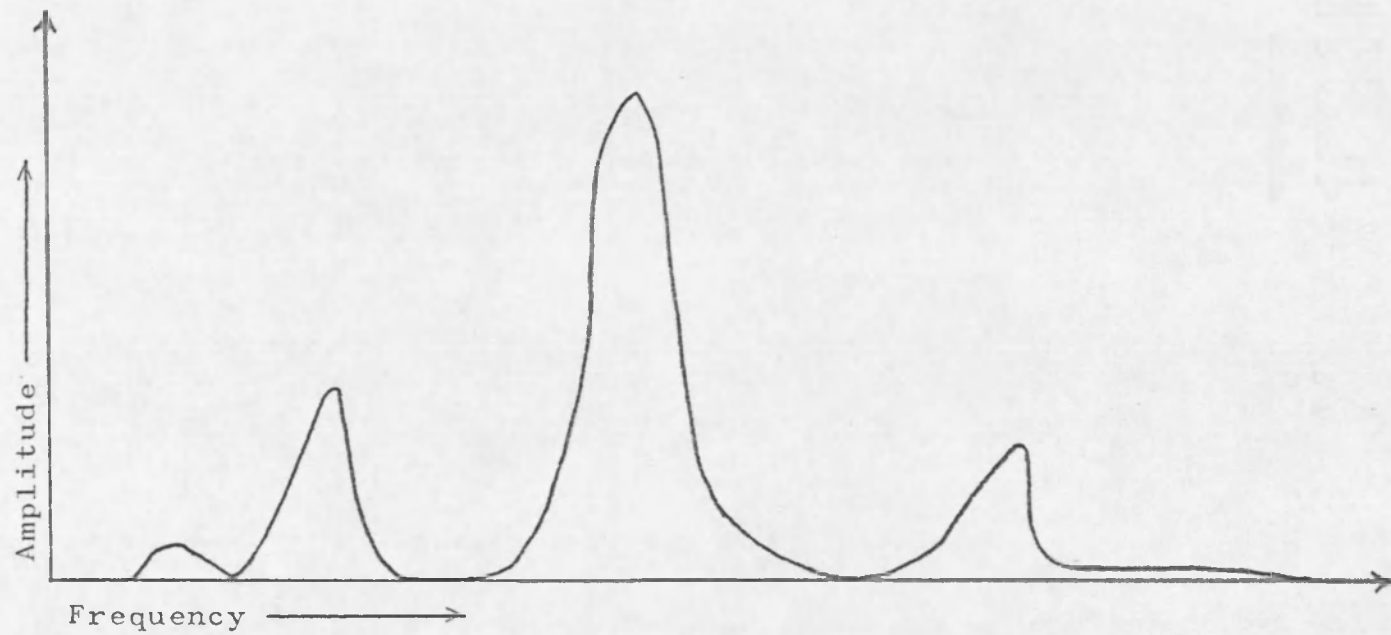


Figure 1. Absorption Spectrum

typical gas with a permanent dipole moment. Thus, if microwave radiation at a constant level were transmitted through a pollutant gas, a graph like Figure 2 should appear at the receiver. If only two frequencies were transmitted (see Figure 2), "A" corresponding to a frequency at which the gas absorbs a maximum of radiation, and "B" at which effectively no absorption takes place at all, then the difference between "A" and "B" would be the amount of absorption due to the pollutant gas. In addition the variation of "A" with respect to "B" would indicate the relative change in concentration of the gas.

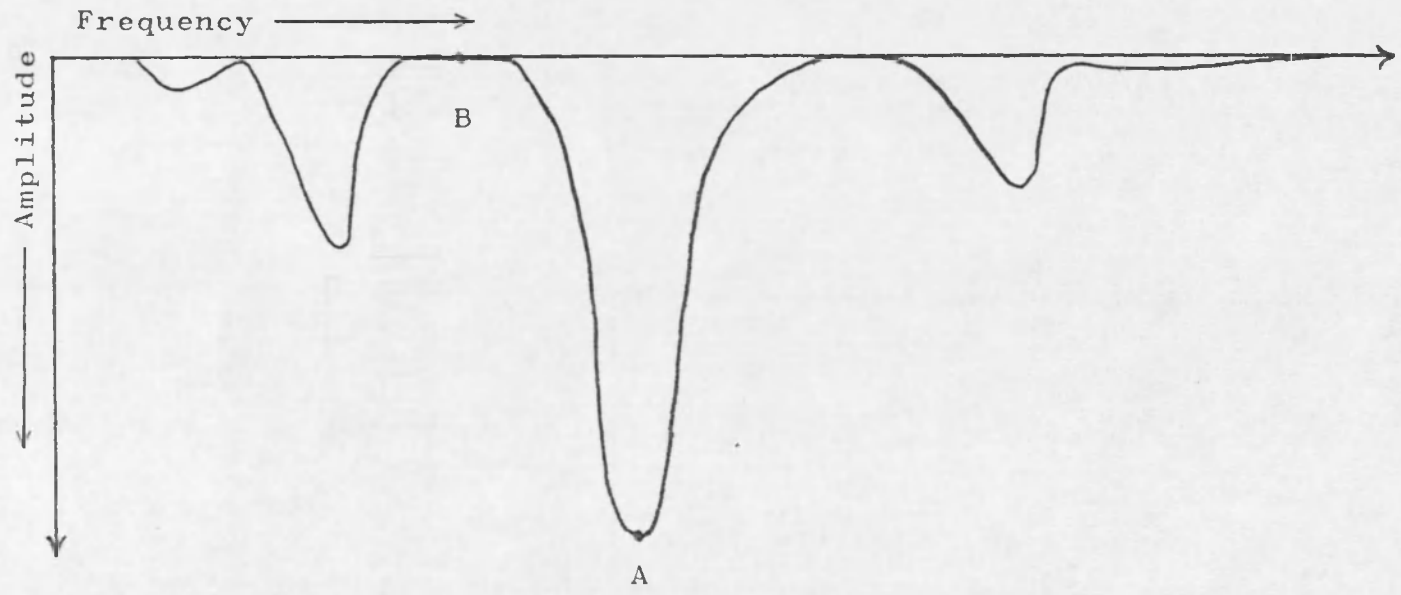


Figure 2. Signal at Receiver

THEORY OF THE MICROWAVE ABSORPTION COEFFICIENT
FOR ROTATIONAL ENERGIES OF GAS MOLECULES

Classical Theory of Molecular Energy
and Absorption

As stated previously in the Introduction, the two experimental facts observed about gases through which microwave radiation is passed are: some of the microwave radiation is absorbed by the gas, and the absorption is frequency dependent.

Since these properties are characteristic of gases in general, they can be most easily understood by examining the simplest type of gas--one consisting of diatomic molecules. Classically the diatomic molecule can be modeled as a rigid dumbbell rotor as in Figure 3. In this model the length between the atoms is considered fixed. When this molecule is given some energy, each atom in the molecule will begin to rotate about a fixed point in the molecule called the center of mass. The energy will be stored in the molecule as kinetic energy of rotation of each of the atoms as given by

$$E_1 = \frac{1}{2} m_1 r_1^2 \omega^2 \quad (1)$$

where m_1 is the mass of the first atom, r_1 is the distance from the center of mass to the first atom, and ω is the

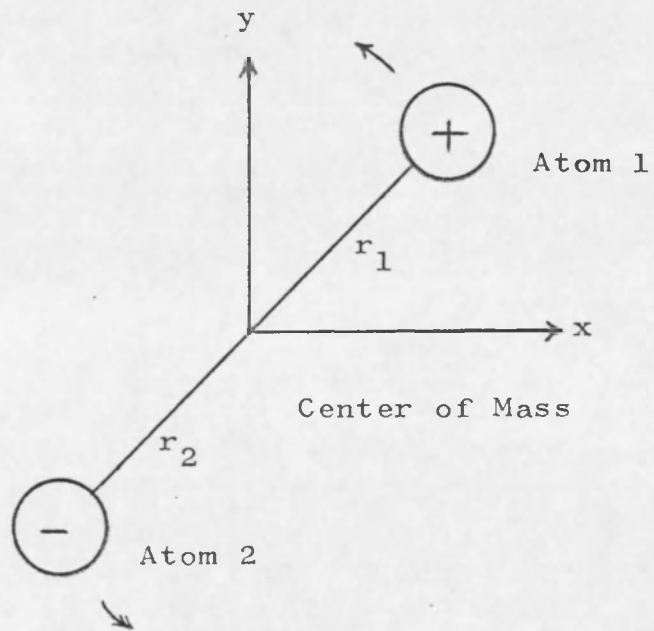


Figure 3. Dumbbell Rotor Model of a Diatomic Molecule

speed of rotation of the atom about the axis through the center of mass. Similarly for the second mass

$$E_2 = \frac{1}{2} m_2 r_2^2 \omega^2 \quad (2)$$

The total kinetic energy of the molecule is just the sum of the kinetic energy of each atom, viz:

$$E_{T_r} = \frac{1}{2} (m_1 r_1^2 + m_2 r_2^2) \omega^2 \quad (3)$$

In Equation (3) let

$$I = m_1 r_1^2 + m_2 r_2^2 \quad (4)$$

where "I" is called the moment of inertia. Substitution of (4) into (3) gives

$$E_{T_r} = \frac{1}{2} I \omega^2 \quad (5)$$

The energy given by Equation (5) could be transferred to the rotor by an interaction of the electric field of the radiation with the dipole moment of the rotor. In this interaction a force

$$\vec{F} = q\vec{E} \quad (6)$$

will be exerted on the charge associated with each mass of the rotor. The resulting torque

$$\vec{\tau} = \vec{\ell} \times \vec{F} \quad (7)$$

or more commonly written

$$\vec{\tau} = q\vec{\ell} \times \vec{E} \quad (8)$$

where "q" is the charge and " $\vec{\ell}$ " is the length between the atoms and " $q\vec{\ell}$ " is defined to be the dipole moment of the molecule. " \vec{E} " is the electric field of the radiation. The torque will cause the molecule to rotate and store energy in the form of kinetic energy of rotation as given by Equation (5). By conservation of energy, this same amount of energy that is stored in the rotor must no longer be present in the wave. Classically, the energy of an electromagnetic wave is related to the square of the amplitude of the electric field of the wave (for a plane wave). After this interaction, the amplitude of the electric field should be less than it was before the interaction.

In the above development, the frequency of the electromagnetic wave did not enter in the calculations. Thus, it appears from the above analysis that electromagnetic radiation of any frequency should interact with the rotor, and the resulting spectrum of the molecule should be continuous with frequency. That is to say, for a wave of constant amplitude, the amount of energy absorbed at one frequency should be the same as at any other frequency. Since the spectra of gases are observed to have discrete rotational energies, this conclusion is not

correct. In order to explain this experimental fact, the above problem must be treated from a quantum mechanical standpoint.

Quantum Theory of Molecular Energy

To simplify a quantum mechanical type of approach for the diatomic molecule the molecule may be shown to be equivalent to a new particle. With this in mind Equation (4) can be rewritten

$$I = \mu r^2 \quad (9)$$

where

$$\mu = \frac{m_1 m_2}{m_1 + m_2} \quad (10)$$

is the mass of the new particle and "r" is the distance between the atoms. Using this form for "I," Equation (5) can be rewritten

$$E_{T_r} = \frac{1}{2} \mu r^2 \omega^2 \quad (11)$$

The form of Equation (11) is similar to Equations (1) and (2) which describe the motion of a single particle around an axis. In the same way Equation (11) can be reinterpreted to describe the motion of a single particle about an axis, but with the advantage that this particle has the same kinetic energy of rotation as the diatomic molecule.

In addition, the location of this single particle can be uniquely related to the position of the diatomic molecule around its center of mass.

Let (x_1, y_1, z_1) and (x_2, y_2, z_2) describe the position of the two atoms of the molecule relative to a fixed coordinate system in space (Figure 4). In addition let (x', y', z') be the coordinates of the new particle where

$$x' = x_1 - x_2 \quad (a)$$

$$y' = y_1 - y_2 \quad (b) \quad (12)$$

$$z' = z_1 - z_2 \quad (c)$$

For each position of the diatomic molecule about its center of mass, the new particle will have a unique position about an axis through the origin of the fixed coordinate system, as seen in Figures 5a, b, c, d. Thus, for the purposes of rotational analysis, the diatomic molecule can be replaced by a single particle of mass μ (for a more quantum-mechanical approach, see Sugden and Kenney, 1965).

If the Schrodinger wave equation for the diatomic molecule is now written in terms of the new particle defined in the last section it will have the following form

$$\frac{h^2}{8\pi^2\mu} \nabla^2 \Psi + (E - V)\Psi = 0 \quad (13)$$

where "h" is Planck's constant in RMKS units (as are all symbols in this paper unless stated otherwise), "E" is the

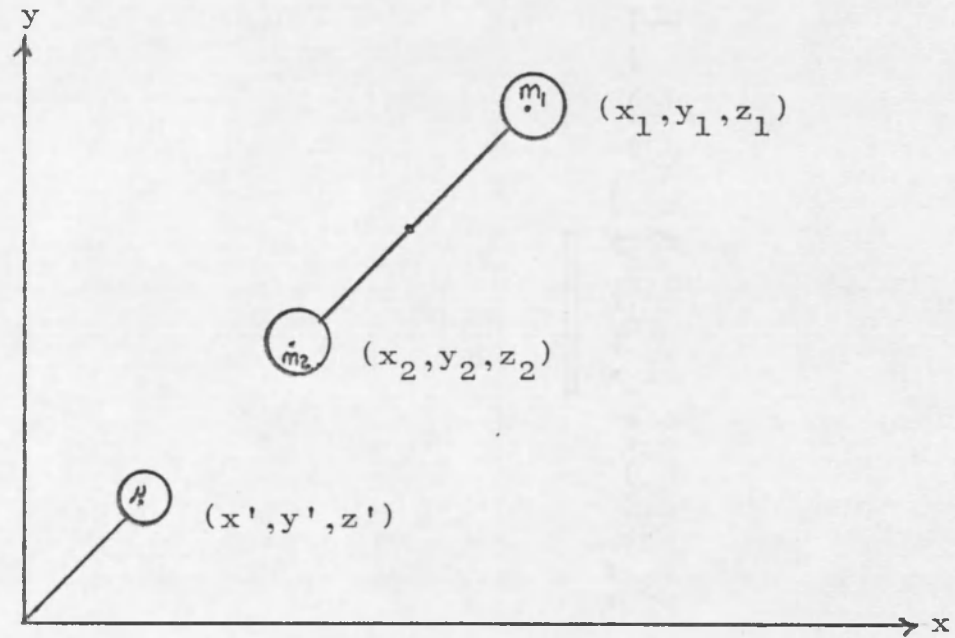


Figure 4. Dumbbell Rotor and Equivalent Particle

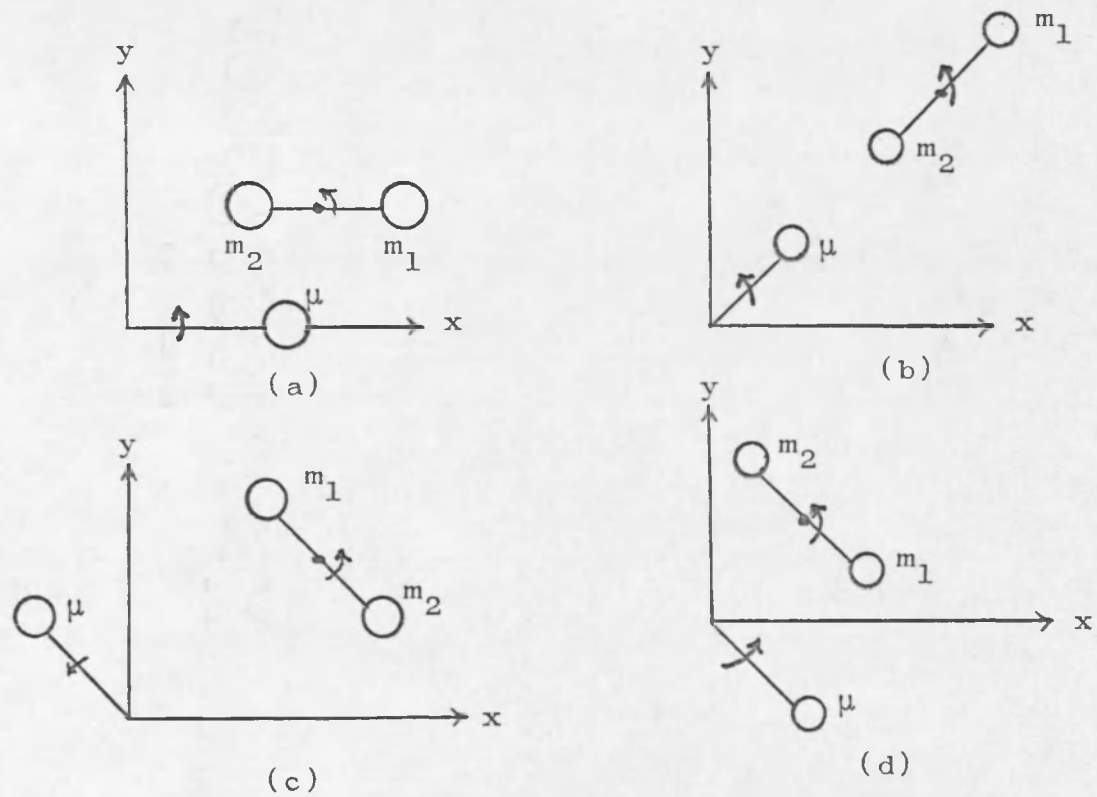


Figure 5. Dumbbell Rotor, Equivalent Particle Positions

rotational kinetic energy, "V" is the potential energy, and " Ψ " is the wave function. If Equation (13) is solved for " Ψ ," " $\Psi\Psi^*dV$ " will give the probability that the new particle will be found in a certain differential volume in space, i.e., in a certain orientation about its axis of rotation. (As mentioned previously the position of this new particle will correspond uniquely to a position of the diatomic molecule.) In addition the rotational energy is found to be quantized. As the rotational energy is increased many different orientations become equally probable. For very large energies " $\Psi\Psi^*dV$ " begins to have a distribution that on the average is independent of angle in space, i.e., all angles are equally probable. For a classical diatomic rotor, turning at a constant speed, any orientation in space is equally likely. Thus, for high energies, the quantum mechanical rotor will behave like a classical rotor. Because this correspondence between classical and quantum mechanical ideas is made at high energy levels, the terminology of the classical model is borrowed when talking about the quantum mechanical rotor. The energy associated with the solution to Schrodinger's equation for this problem is called rotational energy; however, before the correspondence to classical rotation is made, this energy can be designated by any convenient nomenclature. Thus, whether or not something is rotating

is not at all apparent from the solution to Schrodinger's equation.

In the solution of the diatomic rotor constrained to a plane, equation (13) takes the following form

$$\frac{d^2\psi}{d\phi^2} = \frac{-8\pi^2IE}{h^2}\psi \quad (14)$$

where

$$\psi(\phi) = e^{iM\phi} \quad (15)$$

and

$$M^2 = \frac{8\pi^2IE}{h^2} \quad (16)$$

If "M" is required to be single valued, then

$$M = 0, \pm 1, \pm 2, \pm 3, \dots \quad (17)$$

and

$$E_{|M|} = \frac{h^2 M^2}{8\pi^2 I} \quad (18)$$

If "M" can change energy levels by one level at a time, the selection rule will be given by

$$M \rightarrow M + 1 \quad (19)$$

for absorption and

$$\Delta E_M = \frac{h^2}{8\pi^2 I} (2M + 1); M = 0, 1, 2, 3, \dots \quad (20)$$

"M" will be associated with the lower energy state.

Since

$$\Delta E = h\nu \quad (21)$$

$$\nu = \frac{h}{8\pi I}(2M + 1) \quad (22)$$

Let

$$B = \frac{h}{8\pi I} \quad (23)$$

so

$$\nu = B(2M + 1); M = 0, 1, 2, 3, \dots \quad (24)$$

Thus from the quantum mechanical treatment of the rigid rotor problem, it is seen that only those frequencies corresponding to energy differences between energy states will absorb energy. If a band of frequencies of electromagnetic energy is transmitted through a medium containing a diatomic rotor like the one in the above example, absorption will occur at the following frequencies: "B," "3B," "5B," etc. The received spectrum will appear at the receiver as shown in Figure 6.

Therefore it can be seen that to explain adequately the observed experimental facts, the problem must be treated quantum mechanically.

Classification of Gas Molecules

To find the absorption spectrum for an arbitrarily shaped molecule, the Schrodinger equation must in principle

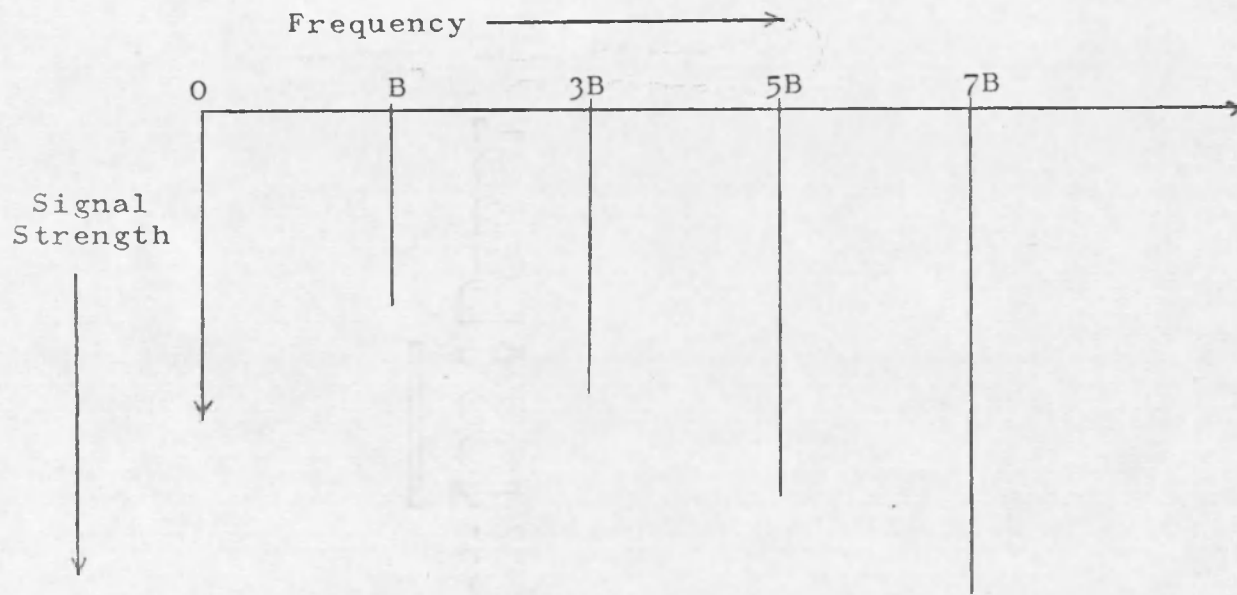


Figure 6. Spectrum of a Diatomic Molecule

be solved for that particular molecule and from the solution the energy levels and transition frequencies determined. This procedure can be greatly simplified, however, if an arbitrarily shaped molecule can be classified according to the general properties of its moment of inertia about certain axes through the molecule. In this way all gas molecules can be classified into two groups--symmetric top molecules or asymmetric top molecules.

An arbitrarily shaped molecule is determined to be a symmetric top or asymmetric top in the following way. Through the center of mass of this molecule draw an axis in an arbitrary direction. About this axis calculate the moment of inertia according to the formula

$$I = \sum_i m_i r_i^2 \quad (25)$$

where "m" is the mass of a particular atom in the molecule and "r" is the distance from the axis to the atom. A distance along the previously chosen axis is then marked off from the center of mass as the origin. This distance is proportional to the moment of inertia previously calculated. This procedure is then repeated for all possible directions through the center of mass. The resulting surface generated is the surface of an ellipsoid or the inertia ellipsoid as it is called in mechanics (Beer and Johnston, 1962). The principal axes of this ellipsoid are

called the principal axes of inertia and the moments calculated about these axes are called the principal moments of inertia. Figure 7 demonstrates graphically the above construction. From the figure it can be seen that the moment of inertia around any arbitrary axis through the mass center will never be greater than one of the principal moments of inertia or less than another principal moment of inertia. The principal axis of a free body has a physical interpretation also. Any free body given a rotation about a principal axis will be in dynamic equilibrium, i.e., will not wobble as it rotates. Using the ideas developed above, molecules are classified according to properties of their inertia ellipsoid and in particular the principal axes. Those gas molecules in which any two principal moments of inertia are the same are classified as symmetric tops. Those molecules in which all the principal moments of inertia are different are classified as asymmetric rotors.

As a simple example of the above ideas consider the diatomic molecule. Two of its principal axes are equal and the third equals zero. Thus it is a symmetric top and its momentum ellipsoid becomes a circle. This is shown graphically in Figure 8 where moment of inertia through any axis in the Y-Z plane is a principal axis.

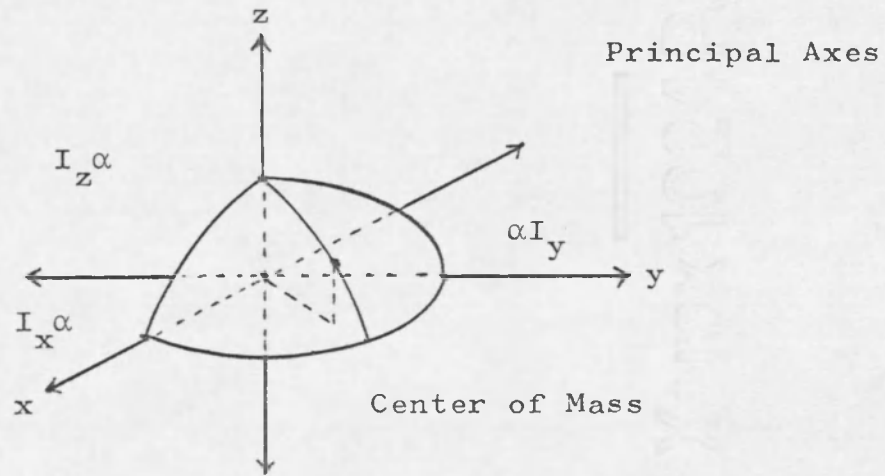


Figure 7. First Octant of the Ellipsoid

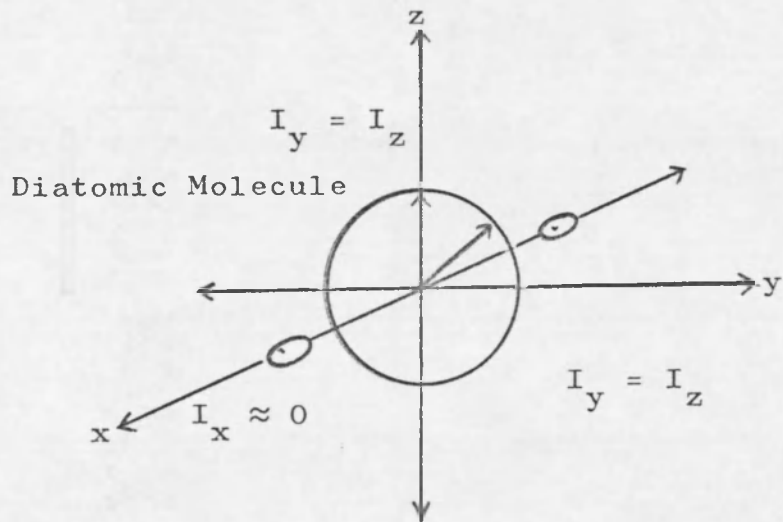


Figure 8. Inertia Ellipsoid of a Diatomic Molecule

Quantum Theory of Molecular Energy Applied
to Classified Molecules

The result of the above analysis is that Schrodinger's equation need only be solved for two appropriate classes and not each individual molecule. The symmetric top molecule was defined to have the same moment of inertia around two of its principal axes. With this restriction, two configurations are possible. If I_A, I_B, I_C are the principal moments then

$$I_A < I_B = I_C \quad (26)$$

defines a prolate symmetric top and

$$I_A = I_B < I_C \quad (27)$$

defines an oblate symmetric top. For the prolate symmetric top the solution to Schrodinger's equation gives an energy term of the following form (Sugden and Kenney, 1965)

$$E_{J,K} = \frac{h^2}{8\pi^2 I_B} J(J+1) + \frac{h^2}{8\pi^2} \left(\frac{1}{I_A} - \frac{1}{I_B} \right) K^2 \quad (28)$$

Let

$$B = \frac{h}{8\pi^2 I_B} \quad (a); \quad A = \frac{h}{8\pi^2 I_A} \quad (b) \quad (29)$$

then

$$v = \frac{E_{J,K}}{h} = BJ(J+1) + (A - B)K^2 \quad (30)$$

where

$$J = 0, 1, 2, 3, \dots \quad (31)$$

and

$$K_J = 0, \pm 1, \dots, \pm J \quad (32)$$

and for the oblate symmetric top (Sugden and Kenney, 1965)

$$v = \frac{E_{J,K}}{h} = BJ(J + 1) + (C - B)K^2 \quad (33)$$

where

$$C = \frac{h}{8\pi^2 I_C} \quad (34)$$

and the other terms are as defined above.

For the asymmetric top molecule, no closed form solution of Schrodinger's equation exists. The energy terms for the asymmetric molecule result from various methods of approximation which are based on the fact that as a molecule becomes less and less asymmetric it becomes more and more like either a prolate or oblate symmetric top. The degree of asymmetry of a molecule is described by its asymmetry parameter (Gordy, Smith, and Trambarulo 1953)

$$\kappa = \frac{2B - A - C}{A - C} \quad (35)$$

The terms "A," "B," "C" are the same ones as defined previously in Equations (29) and (34). For the prolate

symmetric top "B" = "C" and $\kappa = -1$ and for the oblate symmetric top "A" = "B" and $\kappa = +1$. Therefore κ has values between +1 to -1. From the above definition, the "most" asymmetric top would be one in which " κ " = 0. For the general asymmetric top, one method of approximating a solution is by an infinite series of wave function solutions to the Schrodinger equation for the prolate and oblate symmetric top molecules. Since the wave functions for the oblate and prolate cases can be shown to be complete, these wave functions can be used as a basis set to develop the wave functions for the asymmetric case. This method was first used by Ray (in Townes and Schawlow, 1955) and later by King (in Townes and Schawlow, 1955). As a result of this treatment the energy expression for the general asymmetric rotor has the following form (Townes and Shawlow, 1955)

$$v = \frac{W}{h} = \frac{1}{2}(A + C)J(J + 1) + \frac{1}{2}(A - C)E(\kappa)_{K_{-1}K_1} \quad (36)$$

where "A," "B," "C" were defined in Equations (29) and (34) and "J" was defined in Equation (31). $E(\kappa)_{K_{-1}K_1}$ is a term similar to the term of the symmetric top molecule discussed previously (Equations 30 and 33). $E(\kappa)_{K_{-1}K_1}$ depends on the degree of asymmetry κ and the particular prolate and oblate energy levels which are the limiting cases. In Figure 9 a typical energy level for a prolate symmetric top is

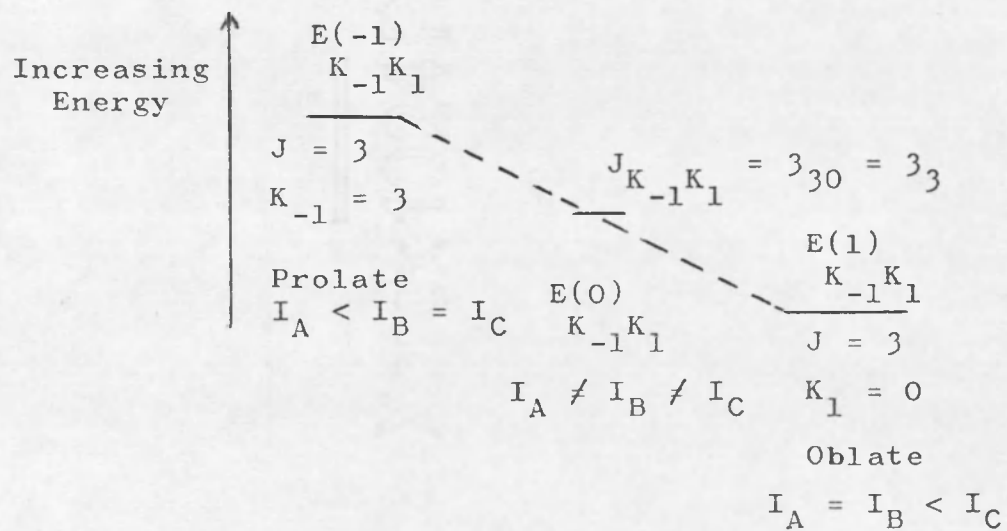


Figure 9. Symmetric, Asymmetric Energy Level

designated by a principal quantum number "J" (Equation 31) and a secondary quantum number "K" (Equation 32). The subscript on "K" indicates that it is a prolate symmetric top molecule. The same explanation applies to the oblate symmetric top except that the subscript indicates the oblate top. This subscript is the limiting case of the asymmetry parameter discussed in Equation (35). By varying κ from -1 to +1, values of $E(\kappa)_{K_{-1}K_1}$ for any degree of asymmetry can be designated unambiguously. In older literature, $E(\kappa)_{K_{-1}K_1}$ is denoted by $E(\kappa)_\tau$ where

$$\tau = K_{-1} - K_1 \quad (37)$$

For low values of κ , $E(\kappa)_{K_{-1}K_1}$ can be expressed as an explicit function of κ . In general $E(\kappa)_{K_{-1}K_1}$ must be calculated numerically. When making calculations using Equation (36), $E(\kappa)_{K_{-1}K_1}$ must be taken from a table (King et al., 1943).

Quantum Theory of Molecular Absorption

With the above discussion as a basis, the quantum mechanical approach can also be used to explain the phenomenon of absorption which was dealt with classically on pages 5 to 9. In the classical approach, the energy transfer from the field was expressed in terms of the torque (Equation 8) produced by the electrical field of the radiation. In the quantum mechanical approach, photons of electromagnetic energy of the correct frequency are

absorbed by the molecules as the photons pass through a layer of the gas. Since the number of photons is proportional to the energy carried by the radiation, the decrease in the number of photons will appear at the receiver as a decrease in power. These ideas can be expressed quantitatively as follows. Let

$$P_{I \rightarrow II} = B_{I \rightarrow II} \mathcal{J}(\nu) \Delta t \quad (38)$$

where $B_{I \rightarrow II}$ is a quantum mechanical proportionality constant and $\mathcal{J}(\nu)$ is the time average power flow (average energy per area per time) of the electromagnetic radiation. $P_{I \rightarrow II}$ is the probability of a transition from energy level I to energy level II (where $E_{II} > E_I$) in time Δt and at frequency ν . Similarly let

$$P_{I \leftarrow II} = B_{I \leftarrow II} \mathcal{J}(\nu) \Delta t \quad (39)$$

be the probability of a transition from II to I in a time Δt and at frequency ν . Let N_I equal the molecular density (molecules per volume) in state I and N_{II} equal the molecular density in state II. Then

$$N_I' = N_I P_{I \rightarrow II} \Delta V \quad (40)$$

will be the number of transitions from state I to state II in a volume ΔV in a time Δt . Similarly for state II

$$N_{II}' = N_{II} P_{I \leftarrow II} \Delta V \quad (41)$$

For each transition from state I to state II, let one photon be absorbed. For each transition from II to I let one photon be emitted. Also assume that the emitted photons are in phase with the incident photons. The net number of photons absorbed in a volume ΔV in a time Δt is then

$$\underline{P}_1 = (N_I^I - N_{II}^I) \Delta V \quad (42)$$

Let "j" be the photon flux (photons per area per time) then

$$\underline{P}_2 = j \Delta A \Delta t \quad (43)$$

will be the number of photons flowing into the volume ΔV in time Δt . The fractional number of photons absorbed in the volume ΔV in time Δt will be

$$\frac{\underline{P}_1}{\underline{P}_2} = \frac{(N_I^I - N_{II}^I) \Delta V}{j \Delta A \Delta t} \quad (44)$$

Substitution of Equations (40) and (41) into Equation (44) yields

$$\frac{\underline{P}_1}{\underline{P}_2} = \frac{[N_I B_{I \rightarrow II} \mathcal{J}(\nu) \Delta t - N_{II} B_{I \leftarrow II} \mathcal{J}(\nu) \Delta t] \Delta V}{j \Delta A \Delta t} \quad (45)$$

From the theory of Einstein transition probabilities (Feynman, Leighton, and Sands, 1963)

$$B_{I \rightarrow II} = B_{I \leftarrow II} \quad (46)$$

also

$$j = \frac{\mathcal{J}(\nu)}{h\nu} \quad (47)$$

Substitution of these additional relations in Equation (45) gives

$$\frac{P_1}{P_2} = h\nu(N_I - N_{II})B_{I \rightarrow II} \Delta X \quad (48)$$

Now, $\frac{P_1}{P_2} h\nu$ is equal to energy. Rearrangement of Equation (43) gives

$$j = \frac{P_2}{\Delta A \Delta t} \quad (49)$$

so

$$S = h\nu j \quad (50)$$

where "S" is the power density. From the above relationships

$$\frac{P_1}{P_2} = \frac{\Delta S}{S} \quad (51)$$

so

$$\frac{\Delta S}{S} = h\nu(N_I - N_{II})B_{I \rightarrow II} \Delta X \quad (52)$$

Since the power density is constant perpendicular to the direction of power flow (plane wave)

$$\frac{\Delta S \Delta A}{S \Delta A} = \frac{\Delta P}{P} \quad (53)$$

and

$$\frac{\Delta P}{P} = -\alpha \Delta X \quad (54)$$

where

$$\alpha = h\nu(N_I - N_{II})B_{I \rightarrow II} \quad (55)$$

Feynman et al. (1963) have shown that

$$B_{I \rightarrow II} = 8\pi^3 \left[\frac{\mu_{I II}^2}{4\pi\epsilon_0 h^2 c} \right] \quad (56)$$

In this form, Equation (56) gives the correct quantum mechanical proportionality constant for a natural line width transition. Because of the effect of collision or pressure broadening, Equation (56) has been shown by Van Vleck and Weisskopf (1945) to be modified by

$$S(\nu, \nu_0) = \frac{\nu}{\nu_0} \left[\frac{\Delta\nu}{(\nu_0 - \nu)^2 + (\Delta\nu)^2} + \frac{\Delta\nu}{(\nu_0 + \nu)^2 + (\Delta\nu)^2} \right] \quad (57)$$

Thus Equation (56) becomes

$$B_{I \rightarrow II} = 8\pi^3 \left[\frac{\mu_{I II}^2}{4\pi\epsilon_0 h^2 c} \right] S(\nu, \nu_0) \quad (58)$$

From the Boltzmann distribution (Barrow, 1966), the relation of the molecular density between states is given by

$$\frac{N_{II}}{N_I} = e^{-h\nu_0/kT} \quad (59)$$

Therefore

$$(N_{\text{I}} - N_{\text{II}}) = N_{\text{I}} - N_{\text{I}} e^{-h\nu_0/kT} \quad (60)$$

and

$$(N_{\text{I}} - N_{\text{II}}) = N_{\text{I}} \left(1 - e^{-h\nu_0/kT} \right) \quad (61)$$

Since $h\nu_0 \ll kT$ at room temperatures in the microwave region

$$(N_{\text{I}} - N_{\text{II}}) \approx N_{\text{I}} \frac{h\nu_0}{kT} \quad (62)$$

Thus substitution of Equations (58) and (62) into Equation (55) gives

$$\alpha = h\nu \left[+ N_{\text{I}} \frac{h\nu_0}{kT} \right] 8\pi^3 \left[\frac{\mu_{\text{I II}}^2}{4\pi\epsilon_0 h^2 c} \right] S(\nu, \nu_0) \quad (63)$$

which simplifies Equation (63), viz:

$$\alpha = \frac{8\pi^3 \nu^2 N_{\text{I}} \mu_{\text{I II}}^2}{ckT 4\pi\epsilon_0} \left[\frac{\Delta\nu}{(\nu_0 - \nu)^2 + (\Delta\nu)^2} + \frac{\Delta\nu}{(\nu_0 + \nu)^2 + (\Delta\nu)^2} \right] \quad (64)$$

Integration of Equation (54) yields

$$P = P_0 e^{-\alpha X} \quad (65)$$

Thus Equation (65) shows that the power level of the incident radiation goes down exponentially with distance.

How fast the exponential decreases depends on α , the absorption coefficient.

Since Equation (64) was derived for an arbitrary molecule, it must be modified for the type of gas molecule under study. As this paper deals primarily with sulfur dioxide, an asymmetric molecule, Equation (64) must be changed for this class of molecules. To aid in this modification, Equation (64) is converted to esu units, as most of the literature in this area uses this system of units. The individual constants of the equation were modified as follows

$$N_I = N f_I \quad (66)$$

where "N" is the total molecular density (molecules per cubic centimeter) and f_I is the molecular fraction in state I. For the asymmetric rotor (Townes and Schawlow, 1955)

$$f_I = \frac{(2J + 1) e^{-h\nu_0/kT}}{\sqrt{\frac{\pi}{ABC} \left(\frac{kT}{h}\right)^3}} \quad (67)$$

and

$$N = 9.68 \times 10^{18} (P/T) \text{ mol./cm}^3 \quad (68)$$

where "P" is the pressure in millimeters of mercury. Also (Townes and Schawlow, 1955; Gordy et al., 1953)

$$\mu_{I, II}^2 = \frac{1}{(2J + 1)} \frac{\mu^2}{3} \lambda(I, II) \quad (69)$$

where μ is the dipole moment of the molecule in debye (10^{-18} esu) and $\lambda(I, II)$ is a modifying factor that is found in the tables of Cross et al. (1944) and has no dimensions. Note: The values in the table have all been multiplied by 10^{+4} . In the absorption equation 10^{-4} will be multiplied in so the values may be entered directly from the table as they are. Substitution of Equations (66) and (69) into Equation (64) yields

$$\alpha = 2.46 \times 10^{-24} \sqrt{ABC} \mu^2 \lambda(I, II) P v^2 e^{-h\nu_0/kT} \cdot \left[\frac{\Delta\nu}{(\nu_0 - \nu)^2 + (\Delta\nu)^2} + \frac{\Delta\nu}{(\nu_0 + \nu)^2 + (\Delta\nu)^2} \right] \text{cm}^{-1} \quad (70)$$

at "T" = 300 degrees Kelvin. Equation (70) can be put in a more useful form in the following way. Let

$$P(X) = P_0 e^{-\alpha X} \quad (71)$$

and

$$\frac{P(X)}{P_0} = e^{-\alpha X} \quad (72)$$

Then

$$10 \log_{10} \frac{P(X)}{P_0} = 10 \log_{10} e^{-\alpha X} \quad (73)$$

and

$$-\frac{10 \log_{10} \frac{P(X)}{P_0}}{X} = +\alpha_{10} \log_{10} e \text{ db/cm} \quad (74a)$$

thus let

$$\alpha_{\text{db}} = +\alpha_{10} \log_{10} e \text{ db/cm} \quad (74b)$$

In this form the absorption coefficient is linear with distance. Because of the large distances involved, the absorption coefficient is usually expressed in decibels per kilometer. Thus in the final form

$$\alpha_{\text{db}} = +\alpha_{10}^6 \log_{10} e \text{ db/km} \quad (75)$$

APPLICATION OF THEORY TO ANALYSIS OF MEASUREMENT FEASIBILITY

From the above absorption formula and the previous information, it is now possible to begin an analysis to see if detection of sulfur dioxide by microwave radiation is plausible. Chemical studies (Mees, 1964) indicate the presence of low concentration levels of sulfur dioxide in the Tucson area. Sulfur dioxide was chosen because it has the type of molecule that can couple through its dipole moment to the electromagnetic field. Also as a pollutant gas, sulfur dioxide has been the subject of much discussion in and around the Tucson area.

Evaluation of Specific Constants of Equation (70) for Use with Sulfur Dioxide

From the chemical studies made on sulfur dioxide in the Tucson area, a minimum and a maximum concentration level has been determined. From these levels, the partial pressure of sulfur dioxide in the atmosphere can be predicted. The average value of this partial pressure is very small, approximately 7.6μ torr. The rotational constants for the sulfur dioxide molecule have been determined from previous spectroscopic studies (Kivelson, 1954) and are easily found in the literature (Townes and Schawlow, 1955). The dipole moment for sulfur dioxide is also readily

available in the literature and from previous studies (Townes and Schawlow, 1955). The modifying term $\lambda(I, II)$ for asymmetric rotors is also available in the form of a table by Cross et al. (1944) as mentioned previously (page 32). Although this information is also reprinted by Townes and Schawlow (1955), the original paper is clearer regarding the correct use of the tables. To find the resonant frequency and the identification of the different energy states between which absorption takes place, the Air Force Surveys in Geophysics (Ghosh and Edwards, 1956) have the most complete listing of microwave resonant lines. This table is also helpful in that resonant frequencies and physical characteristics for other gases are also available. By using the tables given by Townes or the two above mentioned papers, all the information needed for calculation of the absorption coefficient is available.

Effect of Pressure Broadening Parameter

All the unknowns in the absorption equation except one--the half width at half power term $\Delta\nu$ --have been explained. The half width at half maximum power term results from the collision of the sulfur dioxide molecules with other sulfur dioxide molecules and molecules of other gases present. For the case of microwave absorption in the atmosphere, the partial pressure of sulfur dioxide is so low that most of the collisions take place between

nitrogen and oxygen. An exact theory to explain what happens when gas molecules interact is very complicated. These complications result from the fact that the molecules interact with each other at many different distances. The behavior of the molecules at different distances must be explained by different force laws that depend on the separation distances. The different forces possible in a collision are discussed elsewhere (Townes and Schawlow, 1955). As a first approximation to solving this problem, kinetic theory of gases gives a good lower figure for half width of the line--794 MHz (Barrow, 1966). For an upper bound on the parameter, the half width has been shown to vary linearly with the pressure (Gordy et al., 1953), viz.

$$\Delta\nu = \frac{300}{T} P \Delta\nu_1 \quad (76)$$

where $\Delta\nu_1$ is the line width at 300°K and 1 mm Hg and is usually a measured value. Therefore at a temperature of 300°K and a pressure of 760 mm Hg,

$$\Delta\nu = 19 \text{ GHz} \quad (77)$$

Townes (1971) has suggested a value of 3 GHz as a possible value and this value has been adopted by the author as the correct line width parameter.

Because of the lack of a simple theory to explain the collision phenomenon resulting in the values for half-widths discussed above, the half-width is the most

difficult term to account for precisely. For this reason Figures 13 through 17 show the theoretical microwave spectrum of sulfur dioxide as it would appear for different possible half-widths previously discussed. In these graphs the sulfur dioxide is shown mixed with the air to a concentration of about .01 parts per million. This concentration level was chosen because this is the average level of sulfur dioxide present in the Tucson air (Mees, 1964). A study of the above mentioned graphs, and a consideration of some of the other graphs also based on Equation (75) and generated by the computer listing in Figure 10 (Quintenz, 1971), indicate that sulfur dioxide cannot at present be measured by the microwave spectroscopic techniques stated in the introduction.

Cavity Frequency Meter Technique as Applied to Individual Lines

To understand better the basis for the above conclusion it is necessary to examine the individual graphs in more detail. Figure 11 shows the sulfur dioxide spectrum for pure sulfur dioxide as it might be found in a microwave spectroscopic laboratory sample. From this figure two important facts are clear: the individual lines are clearly resolved, and they absorb microwave radiation very strongly. In Figure 12 an enlargement of one of these lines is shown. This line indicates both the high resolution ($\frac{\Delta\nu}{\nu_0} = .001$) and strong absorption (3 db/km) for

```

DIMENSION Z(1,201),ZZ(1,201)
PRINT 99
99  FORMAT (1H1)
DO 47 I=1,201
47  ZZ(1,I)=0.
    PR=.4343*10.**6
    A=60778.8
    B=10318.1
    C=8800.
    PS02=7.6*10.**-6
    U=1.59
    DF=1000.
    DF2=DF**2
    DO 3 N=1,38
    READ 1,J,IZ,E
1   FORMAT(I2,I3,F8.3)
    READ 15,WL,FO
15  FORMAT(F7.0,F9.2)
    P=2.46*(10.**-24)*SQRT(A*B*C)*(U**2)*WL*PS02
    F=10000.
    DO 4 I=1,201
    FC=F
    FD=F-FO
    FDA=ABS(F-FO)
    IF(FDA.LE.700..AND.FD.LE.O)F=FO
    Z(1,I)=P*(F**2)*(DF/((FO-F)**2+DF2)+DF/((FO+F)**2@DF2))
    ZZ(1,I)=Z(1,I)+ZZ(1,I)
    IF (F.EQ.FO)F=FC
4   F=F+700.
3   CONTINUE
    F=10000.
    DO 48 I=1,201
    ZZ(1,I)=ZZ(1,I)*PR
    PRINT 2,I,F,ZZ(1,I)
2   FORMAT (1H ,I4,6X,E15.6,6X,E15.6)
    F=F+700.
48  CONTINUE
    CALL PLOT(ZZ,1,201,100.,1)
    STOP
    END

```

Figure 10. Computer Listing

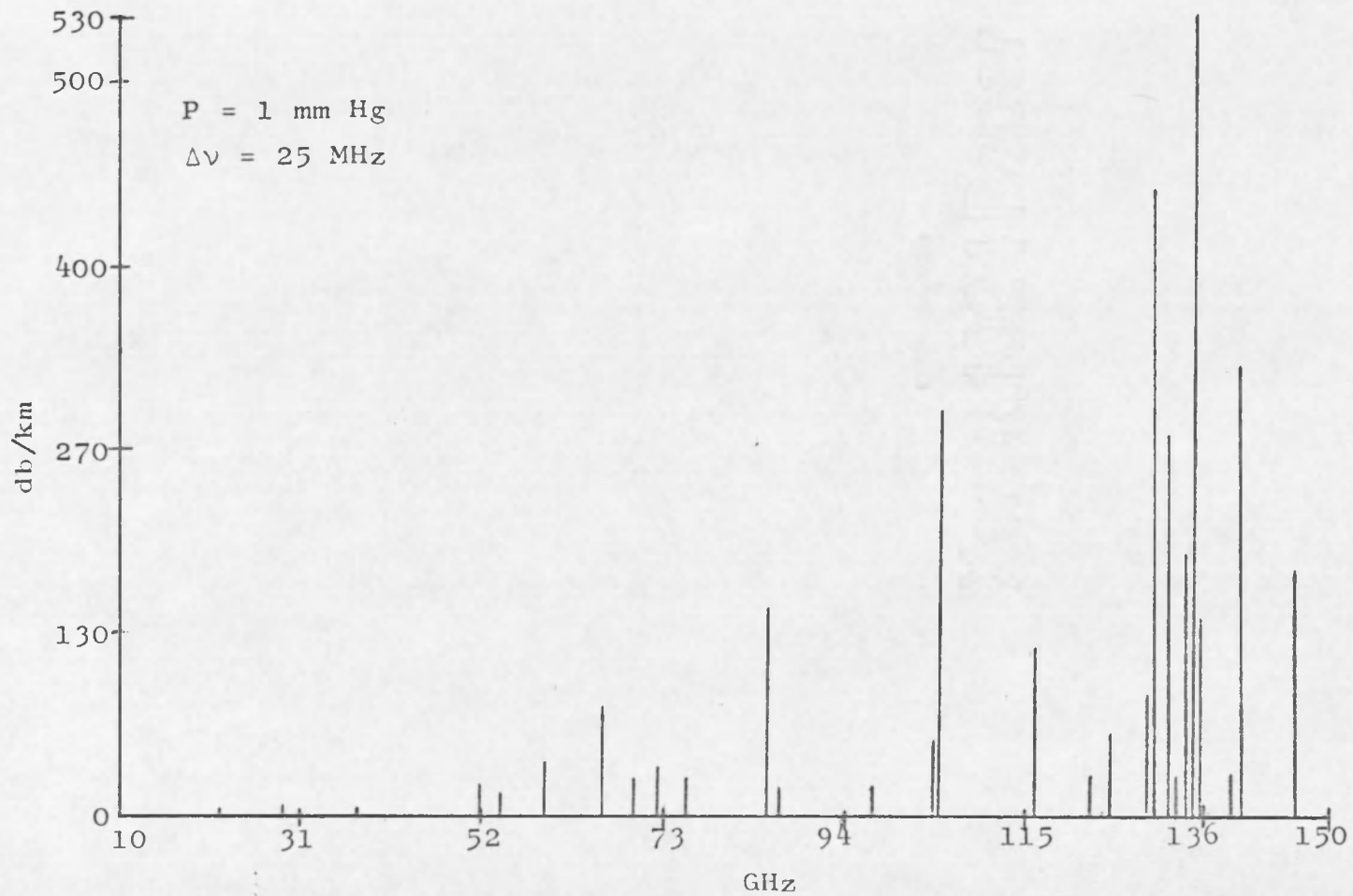


Figure 11. Sulfur Dioxide--Pure Concentration

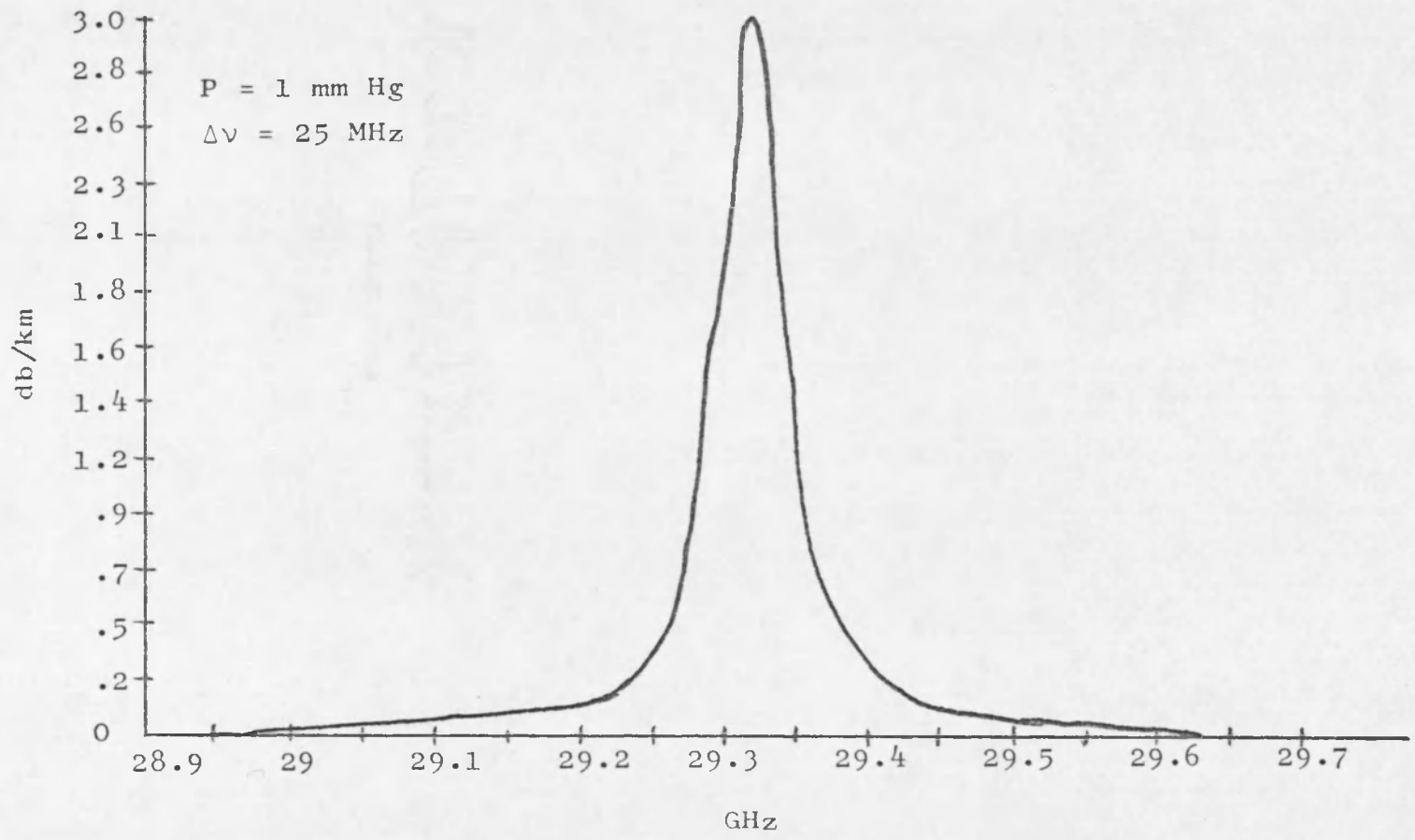


Figure 12. Sulfur Dioxide--Single Line

a typical line shown in Figure 11. The high resolution and strong absorption make the detection of the line very straightforward by conventional techniques (frequency measurement with an absorption cavity frequency meter) (Kosow, 1964). Because of the high resolution of the line ($\frac{\Delta\nu}{\nu_0} = .001$) a very small change in the transmitting frequency would cause the transmitted signal to sweep through the complete line. As the signal passes through the absorption line the large signal change (3 db) is recorded at the receiver.

In Figure 13 the spectrum has been modified to a concentration level of .01 ppm (average concentration for Tucson air). Although the concentration level has been greatly reduced, the individual lines are still highly resolvable. Choosing the strongest line in Figure 13 ($\nu_0 = 134$ GHz) the absorption will be approximately .003 db/km. Although this absorption is very small, the smallest theoretical absorption measurable in a cavity frequency meter measurement is approximately .0004 db/km (Townes and Schawlow, 1955) at a signal level of -40 dbm (a common laboratory signal level in a cavity frequency meter measurement). The .003 db/km given for $\nu_0 = 134$ GHz in Figure 13 represents a much larger signal change than the theoretical minimum detectable value and thus could theoretically be detected.

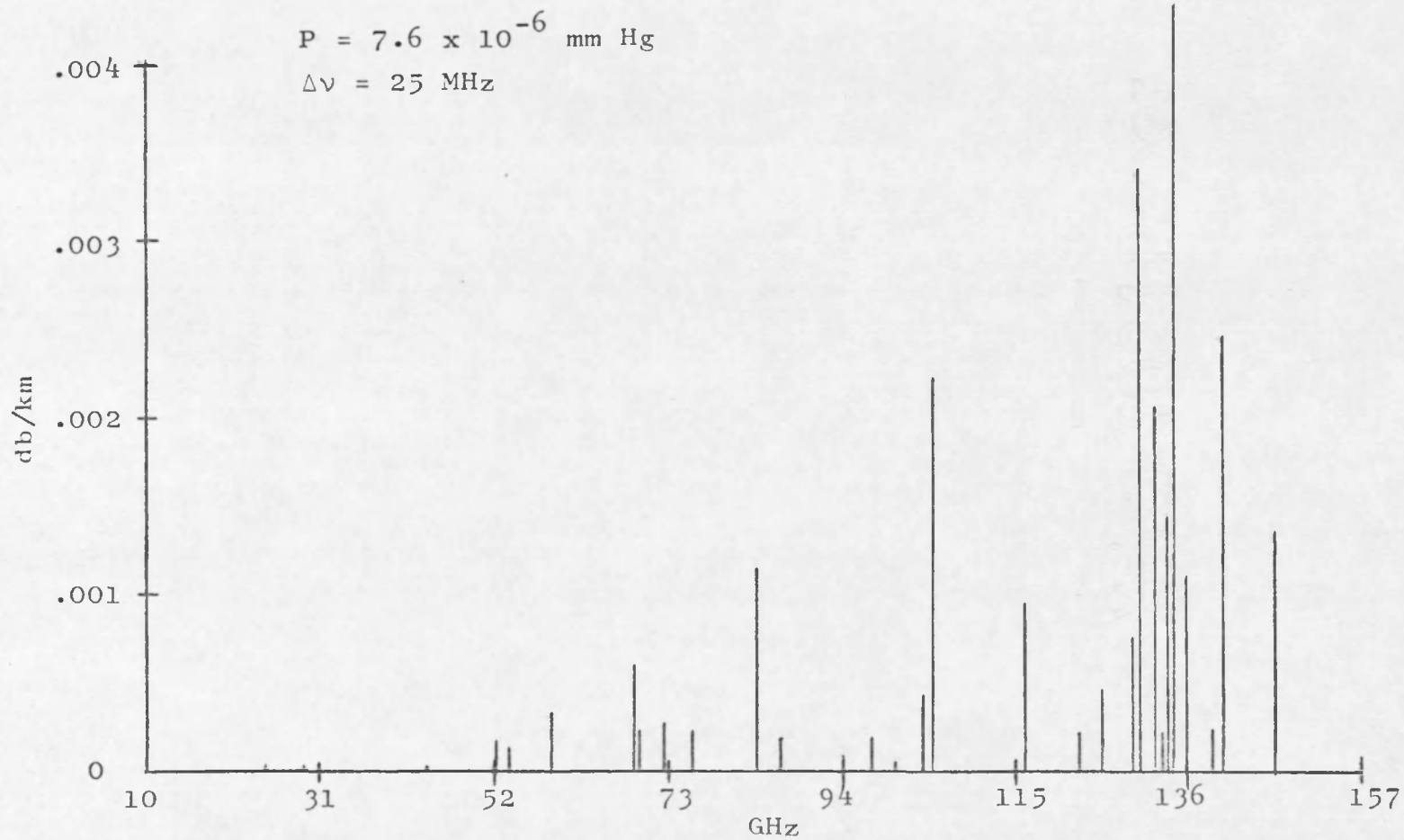


Figure 13. Sulfur Dioxide--0.01 ppm

Although Figure 13 shows the spectrum of atmospheric sulfur dioxide, the effect of collision broadening has not been indicated in this figure. As discussed earlier the collision broadening can vary from 794 MHz to 19 GHz. When the collision broadening effects are added to Figure 13, Figures 14 through 17 result. In these figures the resolution of the individual lines is completely lost. The shape of the spectrums in Figures 14 through 17 results because each individual line in Figure 13 becomes wider, due to the collision broadening effect and, therefore, begins to overlap with other nearby lines. Examination of Figure 14 shows some apparent "lines," but these are the result of the above mentioned overlapping of lines that were close together in frequency. If these apparent "lines" are now considered as the new atmospheric sulfur dioxide "lines" resulting from the collision broadening phenomenon, the cavity frequency meter measurement technique can now be applied to see if it is theoretically possible to measure these new "lines."

Cavity Frequency Meter Technique as Applied to Groups of Pressure Broadened Lines

For purposes of applying the cavity frequency meter measurement technique, the line at $\nu_0 = 134$ GHz shown in Figure 13 will be considered to be a pressure broadened line such as one in Figure 15. It should be emphasized that this "line" does not have a half-width of $\Delta\nu = 3$ GHz,

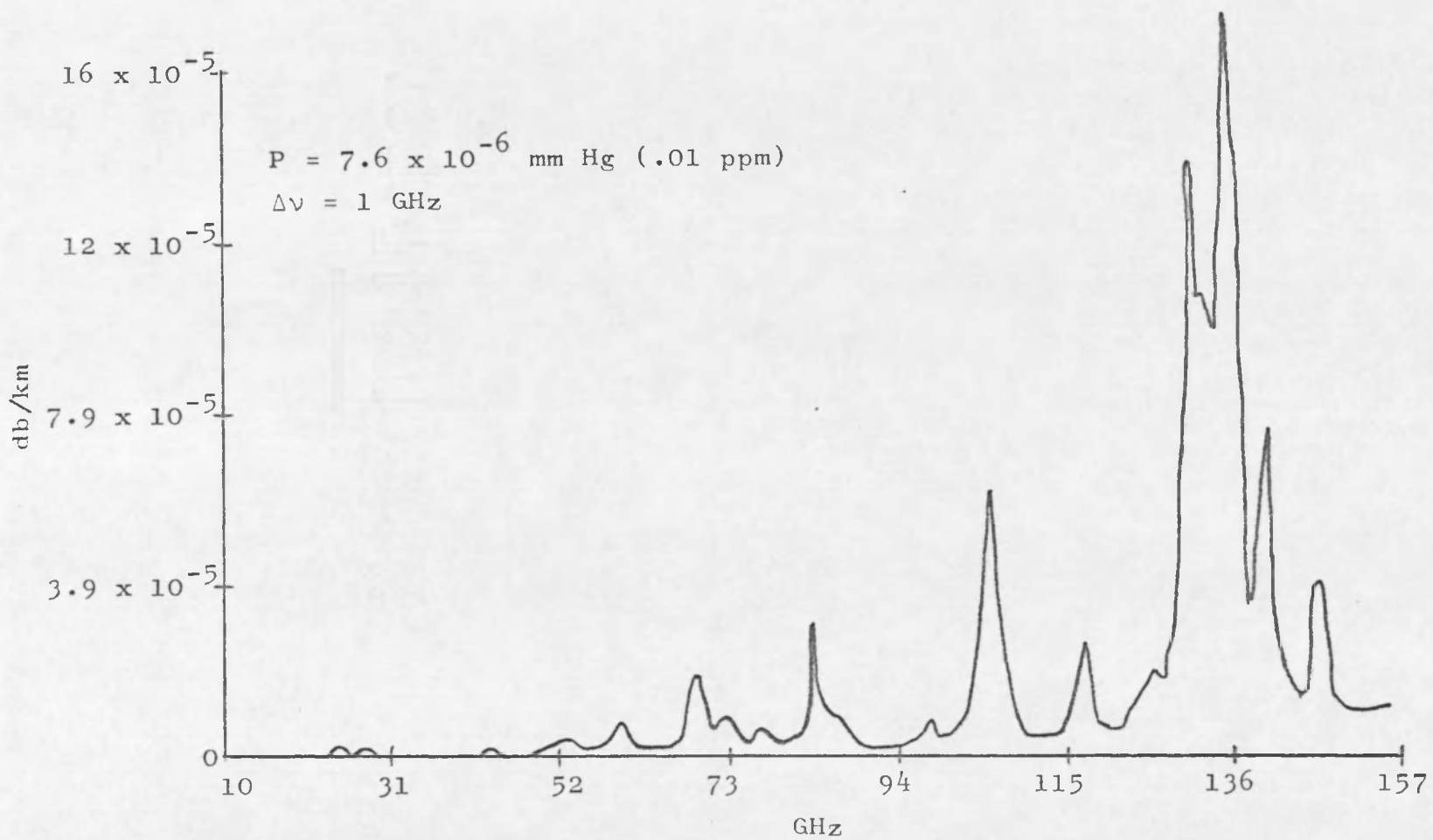


Figure 14. Sulfur Dioxide--Line Width 1 GHz

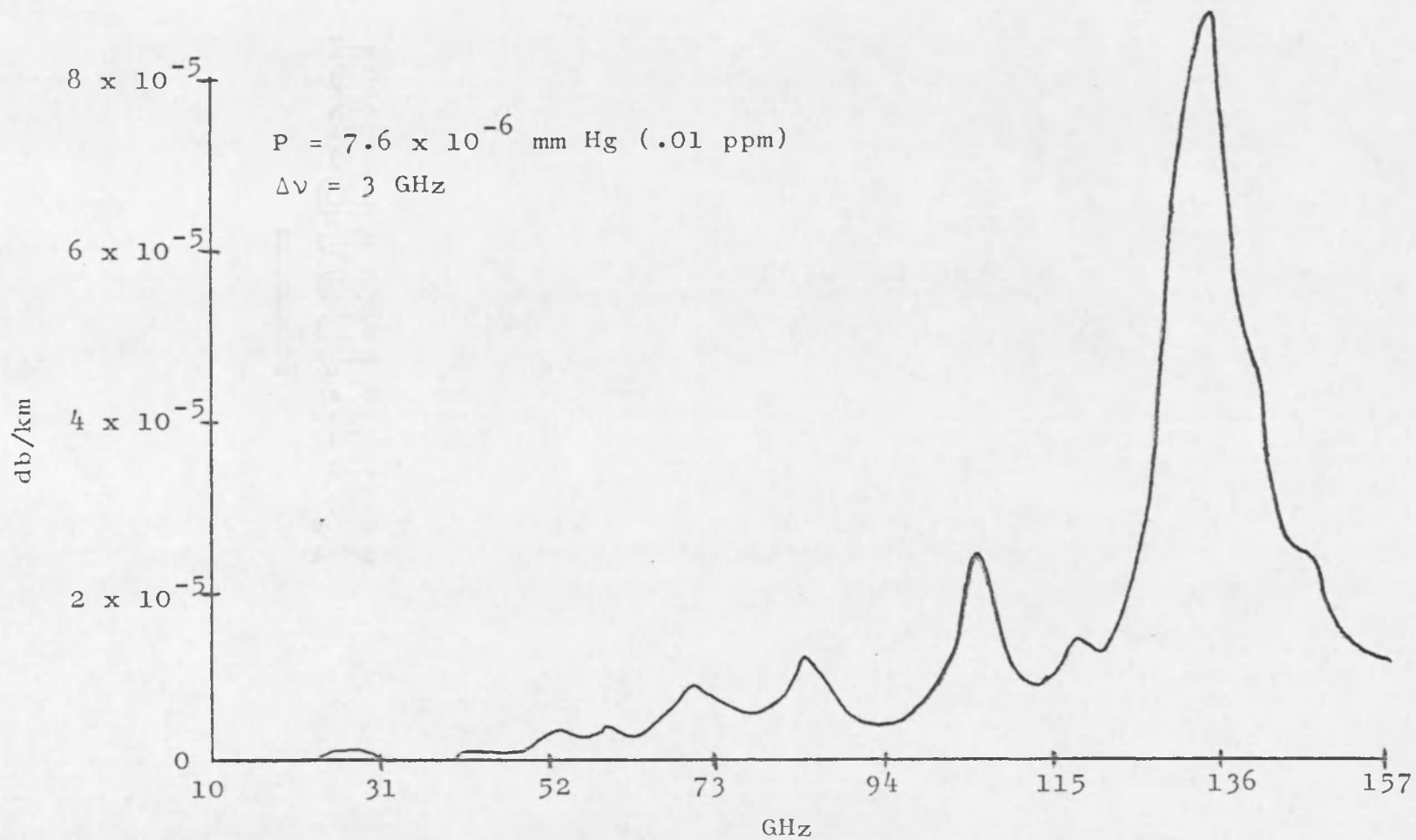


Figure 15. Sulfur Dioxide--Line Width 3 GHz

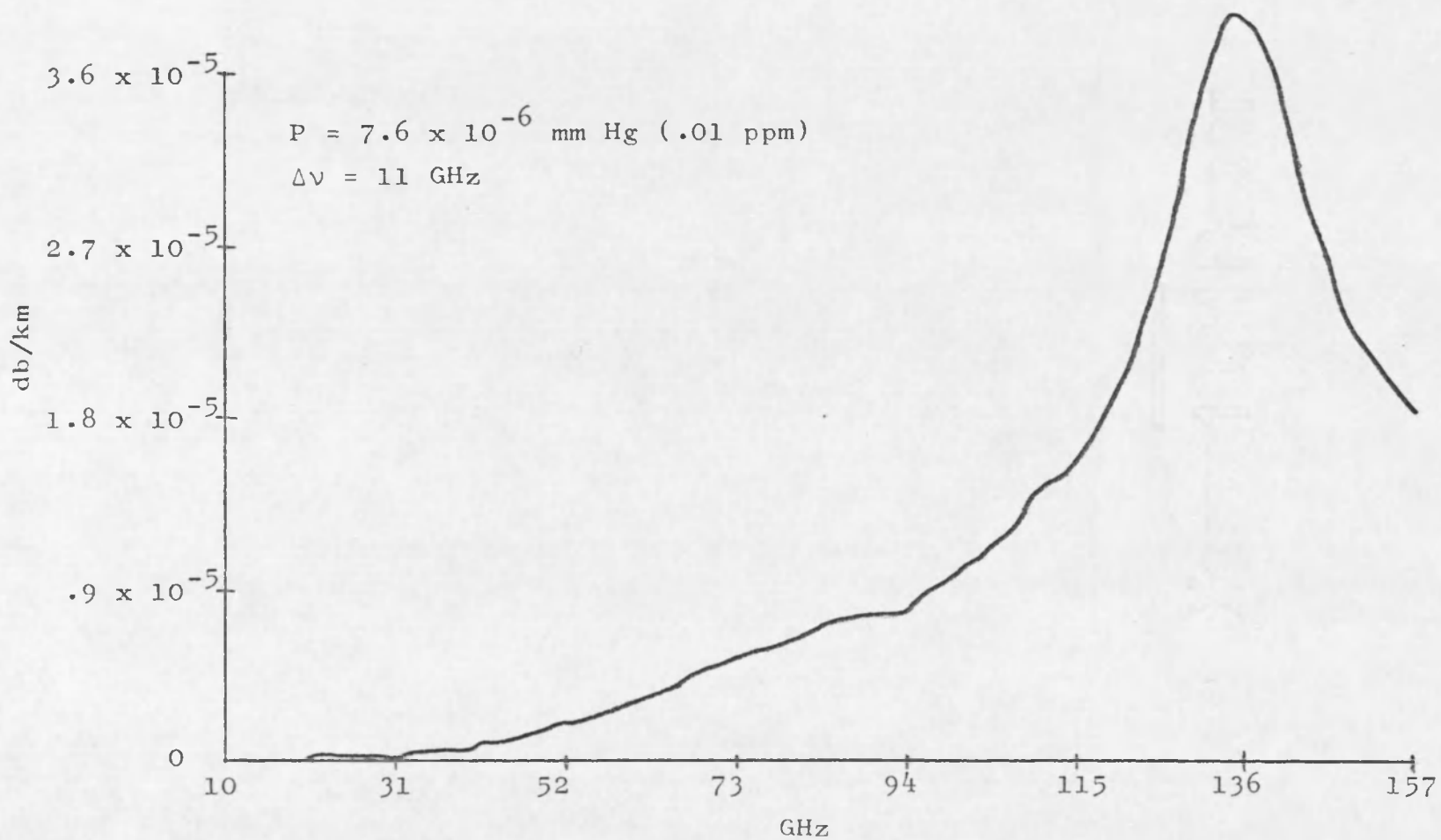


Figure 16. Sulfur Dioxide--Line Width 11 GHz

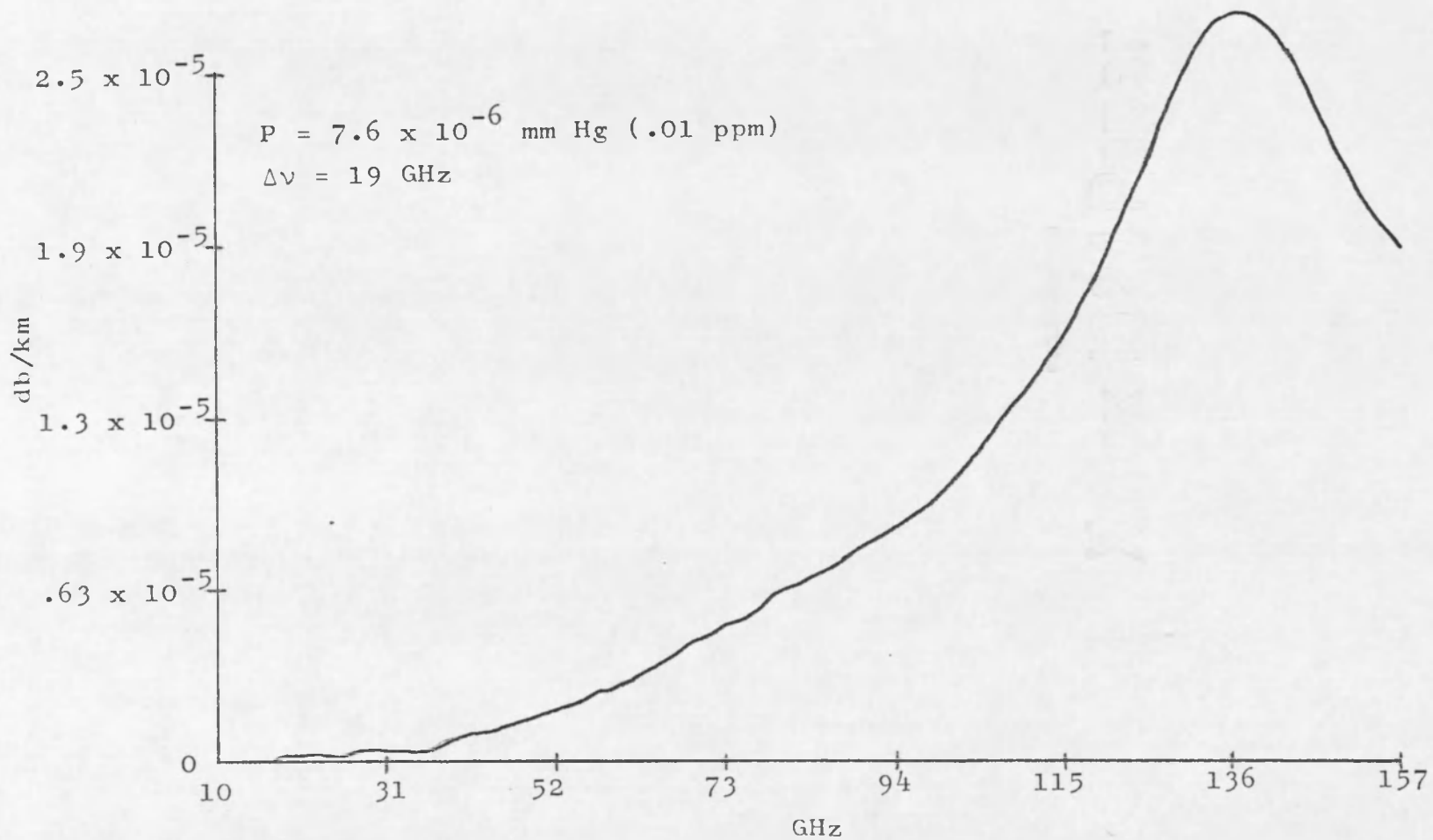


Figure 17. Sulfur Dioxide--Line Width 19 GHz

but rather is the result of the pressure broadening to $\Delta\nu = 3$ GHz of each of the 8 to 10 lines at and around $\nu_0 = 134$ GHz (shown in Figure 13) that resulted in "one line" centered around $\nu_0 = 134$ GHz in Figure 15.

Comparison of this "line" of Figure 15 with the actual line in Figure 13 reveals that the pressure broadened line is approximately an order of magnitude smaller in absorption strength ($\sim .0003$ db/km) and of much lower resolution ($\frac{\Delta\nu}{\nu_0} = .2$) than the unbroadened line of Figure 13.

The smaller absorption strength of this line is of the same order of magnitude as that given by the theoretical limit mentioned earlier for the absorption cavity frequency meter technique. Although stronger concentrations such as those shown in Figures 18 and 19 could eliminate this problem, these small increases represent dangerous and potentially fatal levels of sulfur dioxide concentrations respectively (Mees, 1964) and would thus not be useful for monitoring normal daily concentration levels.

The lower resolution of the line of Figure 15 presents two problems to analysis by absorption cavity frequency meter techniques. One problem is that the signal is not identical for wide frequency variations. This is a problem because the frequency meter technique is based on the following assumption: when measuring the change caused by absorption from a resonant cavity or a gas absorption

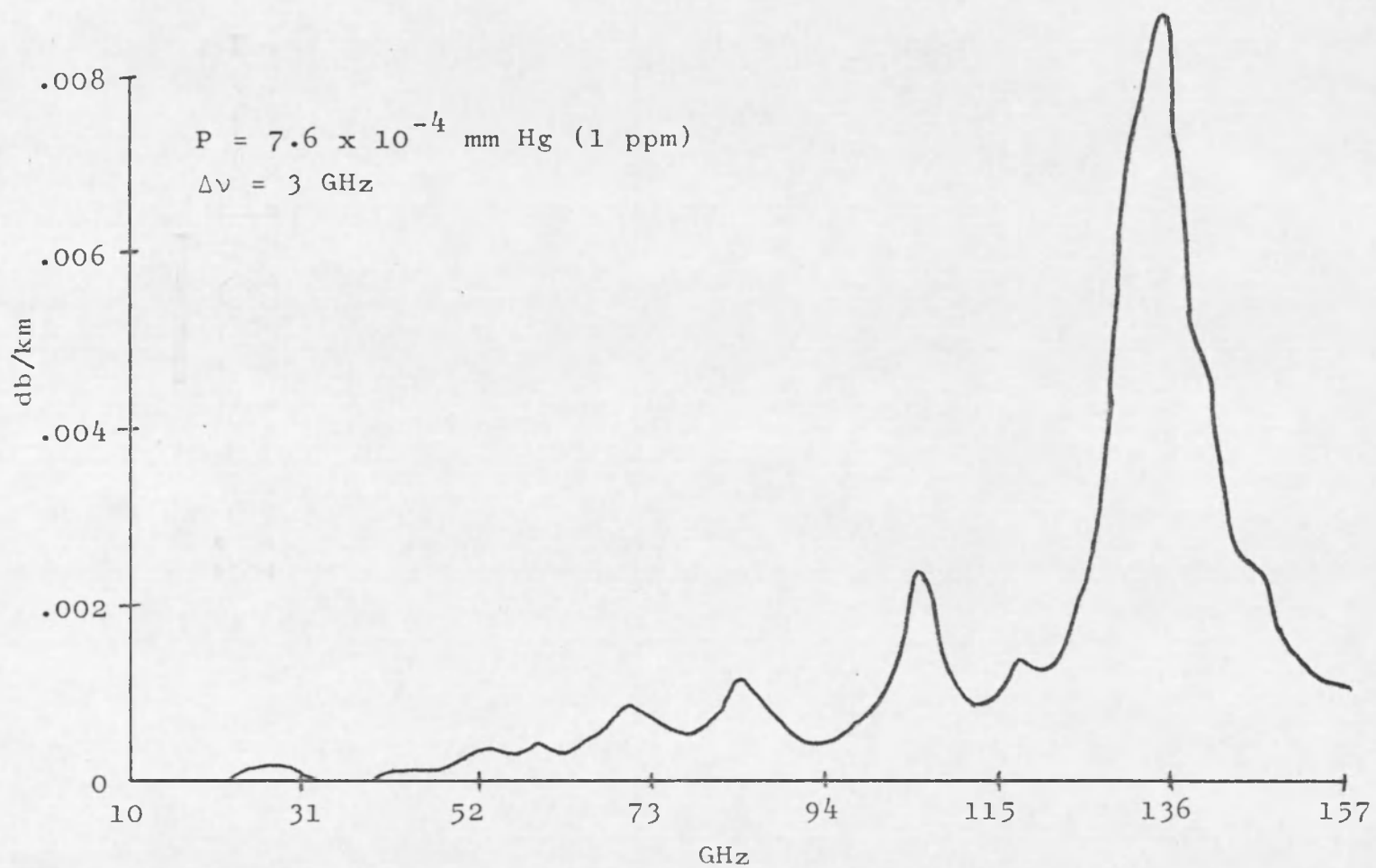


Figure 18. Sulfur Dioxide--Concentration 1 ppm

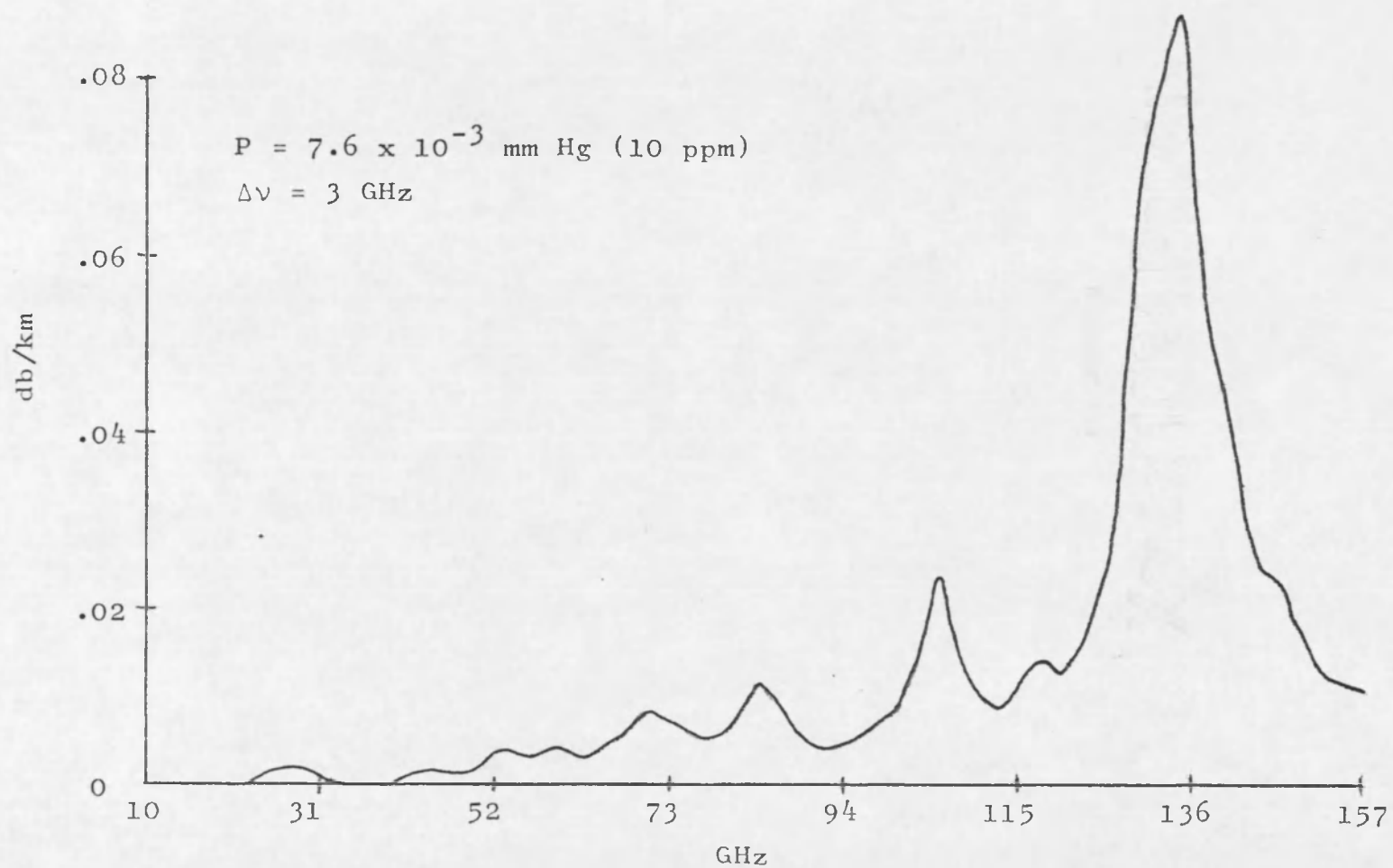


Figure 19. Sulfur Dioxide--Concentration 10 ppm

line, the signal has the same amplitude over the frequency range of interest. Thus if there is a change in amplitude as the signal is swept over a frequency band, the amplitude change is assumed to have occurred as a result of the absorption at a particular frequency by the cavity frequency meter or an absorption line only. When working in the laboratory this assumption is always made over small frequency bands. In using this technique in an atmospheric measurement, the author has also assumed that over small frequency bands (implying high resolution) the effects of fading and absorption from water vapor and oxygen would be the same on the transmitted signal. Thus for a high resolution line of sulfur dioxide these effects would subtract effectively and the amplitude change would be an indication of the sulfur dioxide present. These assumptions resulted from the experimental measure of the fading effects (Roche et al., 1970) and as seen by Figure 20 (Angelakos and Everhart, 1968), over very small bandwidths (25 MHz) the absorption from water vapor and oxygen is essentially constant. For a low resolution line greater bandwidths must be swept over. As a result of this, the signal can no longer be assumed identical. Fading and absorption from water vapor and oxygen become different at different frequencies. Thus, when a signal at two different frequencies is subtracted it can no longer be assumed

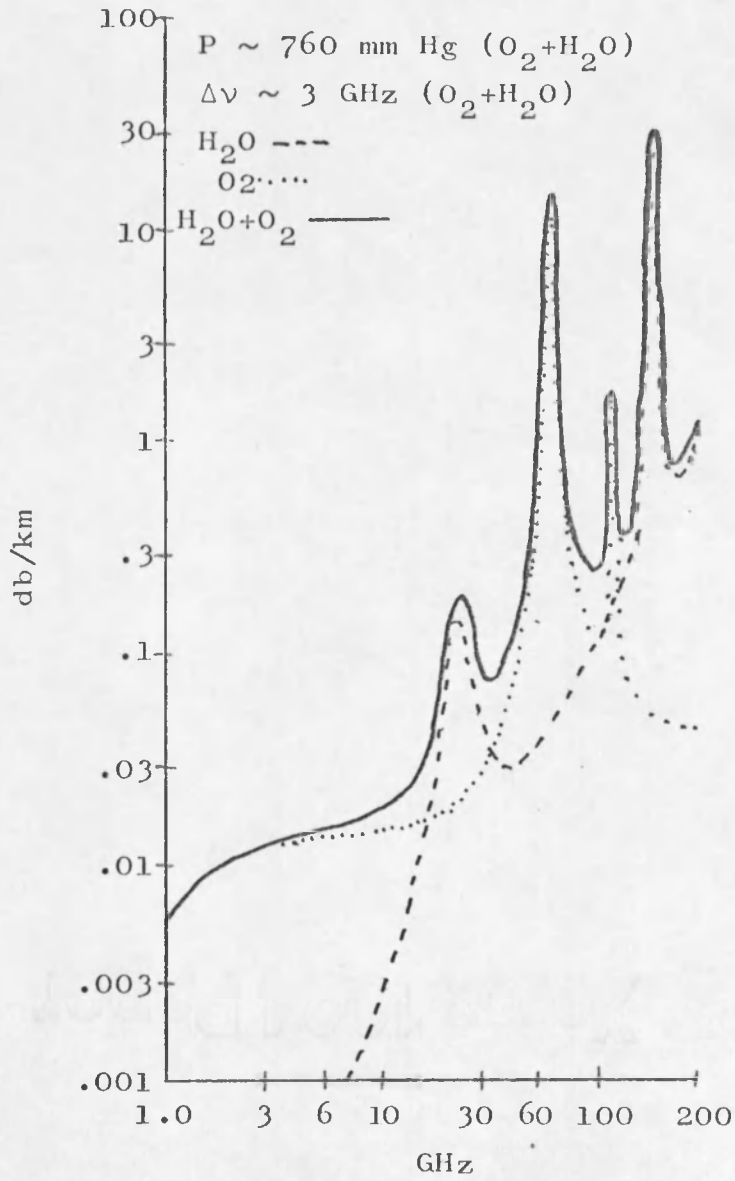


Figure 20. Spectrum of H_2O and O_2

that the difference results only from absorption by sulfur dioxide.

The second problem, resulting from low resolution lines, is that transmitter-receiver equipment with greater bandwidth requirements is necessary. For the above mentioned resolution ($\frac{\Delta\nu}{\nu_0} = .2$) a transmitter with a sweeping capability of 20% of 134 GHz would be required. In addition a receiver capable of "tracking" the transmitted signal would also be needed. To the best of the author's knowledge no such transmitting receiving system is currently available at this frequency ($\nu_0 = 134$ GHz). In addition, if the collision broadening effect were greater than $\Delta\nu = 3$ GHz, lines like those of Figures 16 and 17 might be more representative of the spectrum, and would require equipment with sweep widths even greater than 20%.

In summary, therefore, the small absorption strength of the line and the low resolution clearly indicate that measurement by an absorption cavity frequency meter technique would not be feasible for this type of measurement, and if the measurement is to be made at all, it would require a very complex signal analysis scheme.

EXPERIMENT CONCERNING FEASIBILITY OF MEASURING SULFUR DIOXIDE

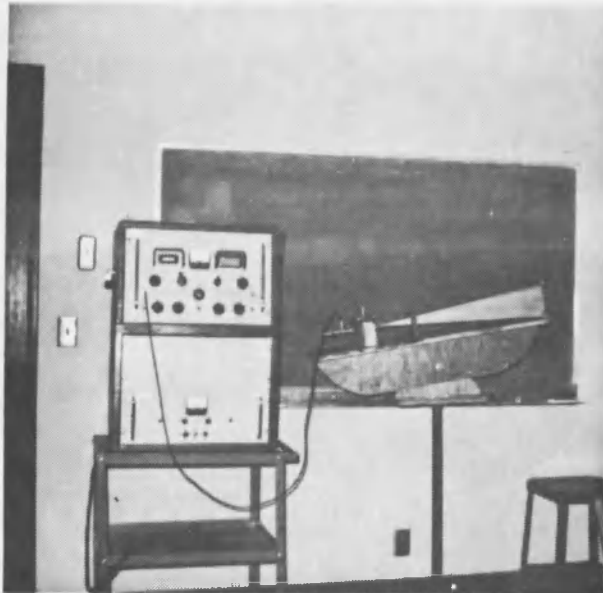
Because much time was spent in the preparation of the previously discussed figures, it was not known until near the end of the program whether or not the sulfur dioxide spectrum resembled Figures 11, 13, or 15. For this reason a second approach to the problem was initiated. At the start of this investigation preliminary study seemed to indicate that the sulfur dioxide spectrum resembled Figure 11. Based on this assumption a simple experiment was set up to try and prove or disprove this assumption. In addition it was hoped that the data gathered from this experiment would eventually supplement the theoretical work that was going on at the same time and at the very least establish the feasibility of measuring sulfur dioxide in the air by an absorption cavity frequency meter technique.

The experiment was of the following nature. A transmitter and receiver were set up at a certain fixed distance (4.85 km) from each other. The transmitter was tuned through a resonant frequency for sulfur dioxide and the resulting dip was anticipated on the receiver. Indication of a dip at the resonant frequency would indicate the presence of sulfur dioxide in the air. The transmitter used in this experiment was built at The University of

Arizona. The heart of the transmitter was a reflex klystron oscillator (Meierdierks, 1970) that generated about +20 dbm of power. The oscillator was isolated and matched to a horn antenna with a gain of 30 db.

The antenna was also built at The University of Arizona. Some of the power generated by the klystron was tapped off through a directional coupler and used to run a frequency meter. In this way a continuous indication of the operating frequency and signal level was possible. A variable attenuator was also inserted between the klystron and the transmitting antenna; and by varying the attenuation, the minimum detectable signal could be determined at the receiver. The entire transmitter was mounted on a stand that was portable and could be disassembled into three parts. In this configuration the transmitter could easily be placed in the back of a station wagon. The entire transmitter could be carried a section at a time by one person. The only piece of equipment connected with the transmitter that was not portable was the power supply for the klystron. The power supply weighed approximately 200 pounds and was left in the station wagon at all times. In the pictures (Figure 21), the main components described above are visible. The receiver was also a very simple device. It consisted of a receiving antenna that was exactly like the antenna used for transmitting. The antenna was connected through the proper matching elements

Receiver



Transmitter

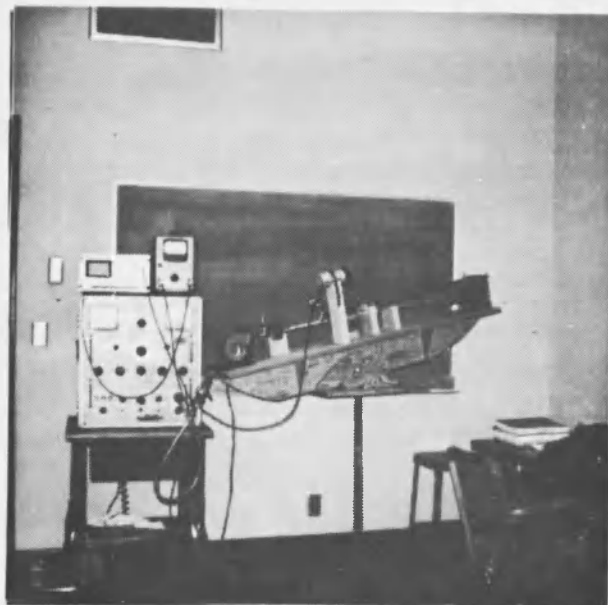


Figure 21. Transmitter-Receiver System

to a crystal mixer. The output from the crystal mixer was connected to an Antlab antenna receiver with an MDS of -70 dbm. Because the conversion from rf to if was done in the crystal it was possible to set up the receiving antenna about 75 feet from the receiver. This feature was useful because it allowed greater flexibility in the placement of the receiving antenna relative to the transmitting antenna. Block diagrams of both the receiver and transmitter are shown in Figures 22 and 23 respectively.

The transmitting antenna was set up on Tumamoc Hill in southwest Tucson, and the receiving antenna was placed on the northwest corner of the PMM building on campus (see Figure 24). The 3 db points of the antennas were such that there was a clear line of sight between these locations both horizontally and vertically for 2.5° either side of a line joining the two sites. The klystron was operated at a frequency of 29.321 GHz as this was a strong resonant line for sulfur dioxide (see Figure 11). In addition this line appeared to be isolated from the absorption lines of other atmospheric gases as seen in Figure 25 (Ghosh and Edwards, 1956).

In Table 1 a summary of the experimental specifications is listed. The data in this table were tabulated in the following way. From antenna theory (Silver, 1965) it is known that the power at a receiver is related to the power at the transmitter by the following equation



Figure 22. Receiver System--Block Diagram

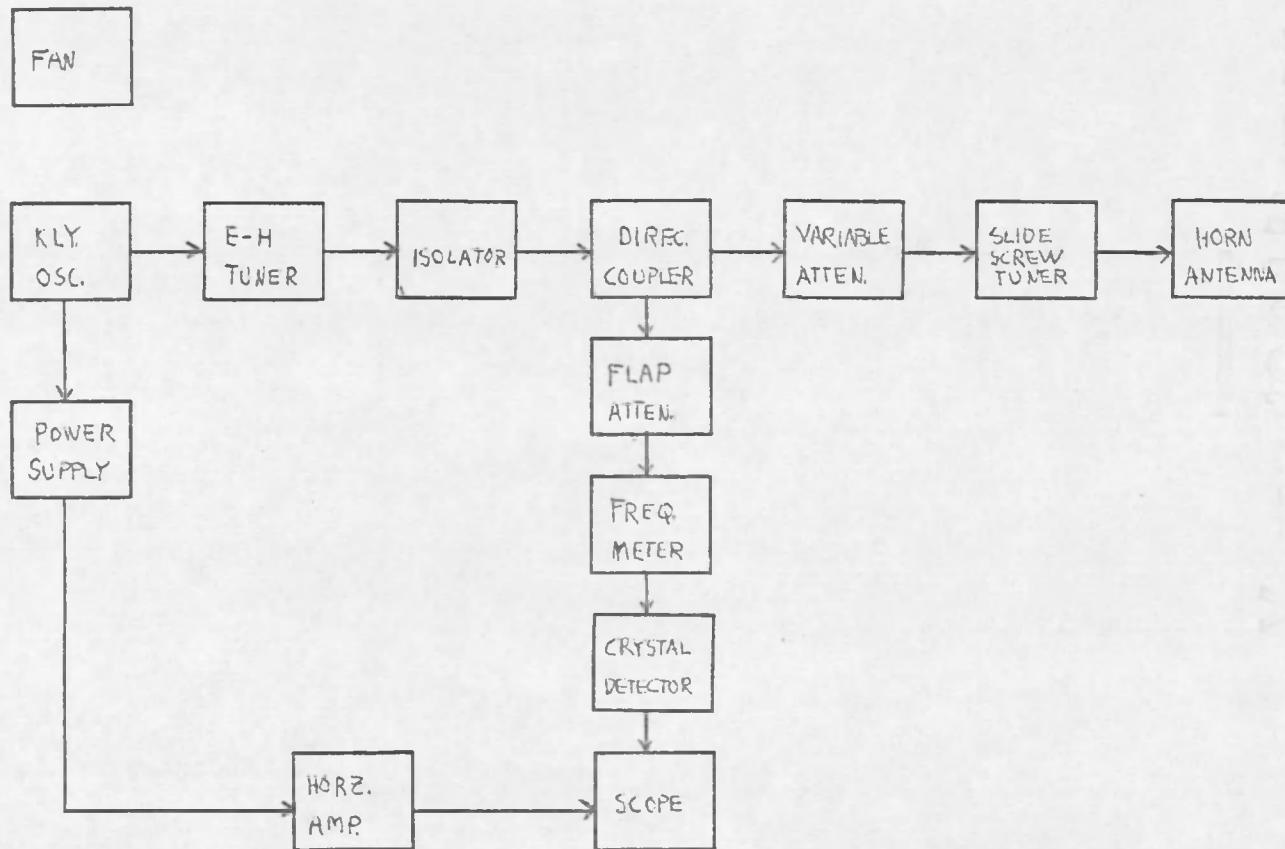


Figure 23. Transmitter Block Diagram

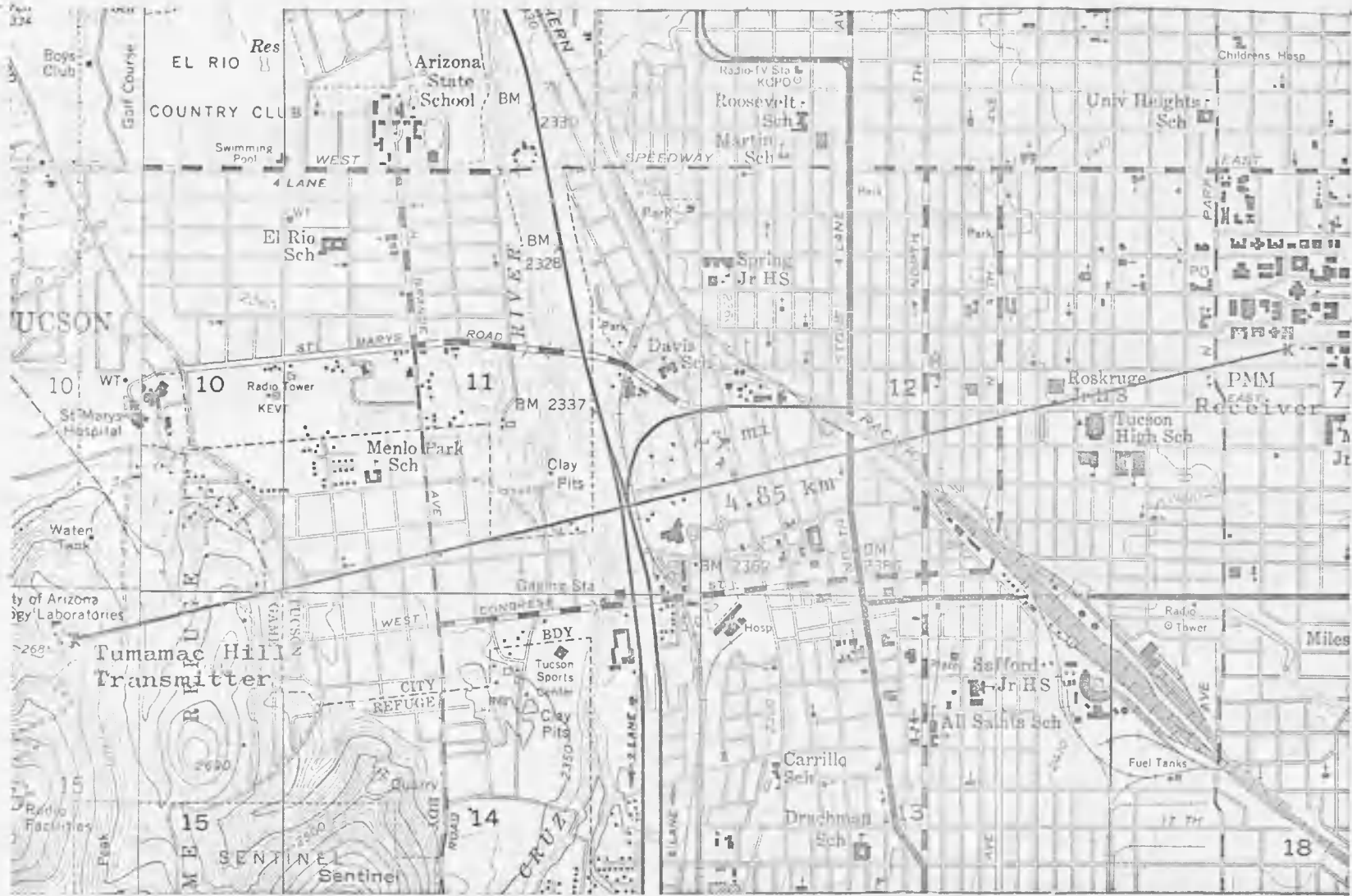


Figure 24. Link Map

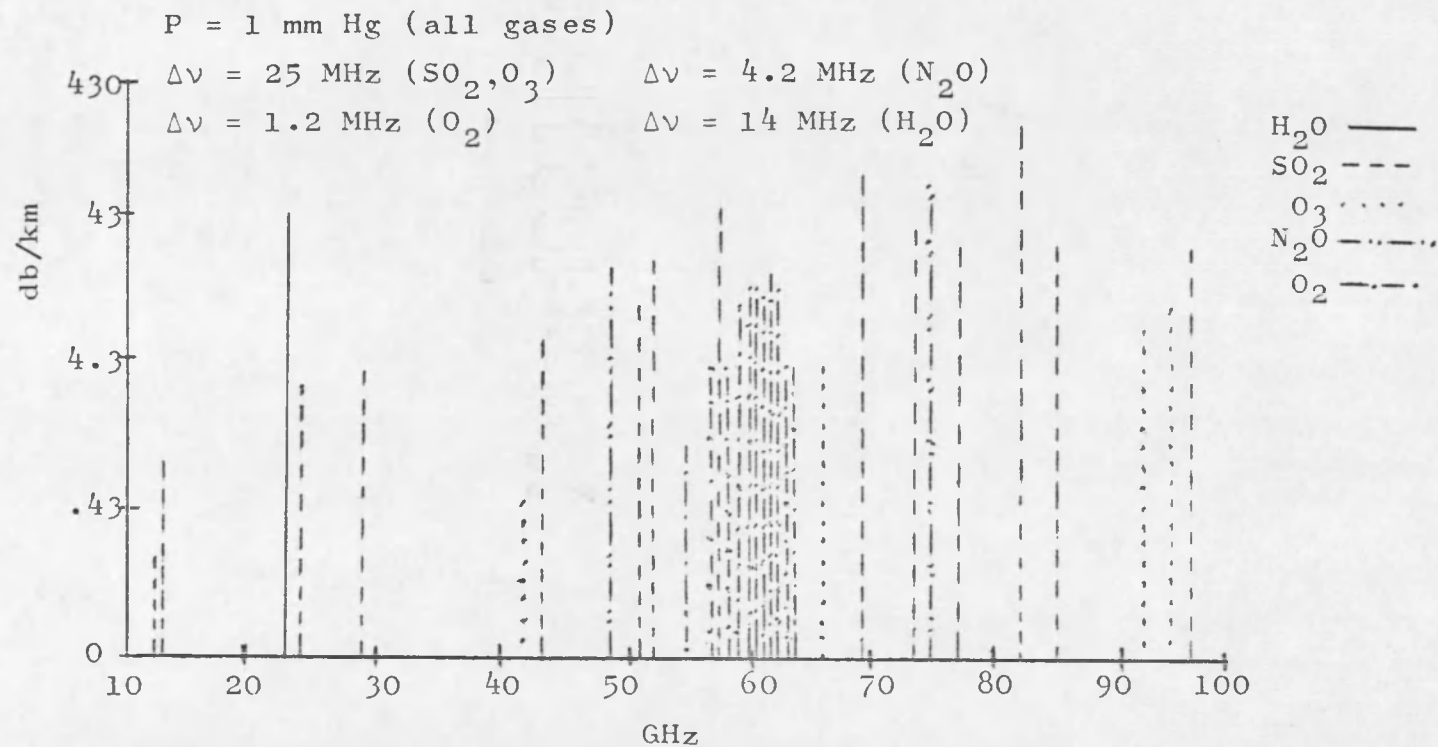


Figure 25. Atmospheric Spectrum

Table 1. Summary of Transmitter-Receiver System Specifications

+20 dbm	=	power into transmitting antenna.
+30 db	=	gain of transmitting antenna.
-137 db	=	free space loss.
+30 db	=	gain of receiving antenna.
-57 dbm	=	power at receiver.
-70 dbm	=	Minimum Detectable Signal (MDS).
-13 db	=	margin.

$$P_r = P_T G_T G_r \left[\frac{\lambda}{4\pi R} \right]^2 \quad (76)$$

where P_r is the power received, P_T is the power transmitted, G_r, G_T , the gain of the receiving antenna and transmitting antenna respectively, λ is the wavelength, and R is the distance between the transmitter and receiver. If this equation is written in decibels it becomes

$$P_{r\text{dbm}} = P_{T\text{dbm}} + G_{T\text{db}} + G_{r\text{db}} + F_{L\text{db}} \quad (77)$$

where $F_{L\text{db}}$ is the free space loss

$$F_{L\text{db}} = 20 \log_{10} \frac{\lambda}{4\pi R} \quad (78)$$

From Equation (77) and the parameters of the experiment it is found that $P_{r\text{dbm}} = -57$ dbm. The margin of a receiver is defined as how much the signal level can decrease and still be received

$$M = \text{MDS} - P_{r\text{dbm}} \quad (79)$$

where M is the margin and MDS is the minimum detectable signal at the receiver. For this particular experiment the margin is -13 db. From Table 1 it can be seen that a dip as large as 13 db could be detected by this experimental system. Moreover at the other extreme a dip of .01 db could be detected with certainty (Leavitt, 1971) for a line of high resolution. Even for a line of high resolution

such as in Figure 13, however, the receiver system would not detect the line at $\nu_0 = 29.321$ GHz. At $\nu_0 = 29.321$ GHz the signal is attenuated approximately .00002 db/km as is seen from Figure 13. At the distance between the receiver and the transmitter (4.85 km) this means a signal decrease of approximately .0001 db resulting from sulfur dioxide. As mentioned earlier the smallest change detectable by the receiver used in this experiment was .01 db for the above path length (4.85 km). Thus since the change in the signal strength resulting from sulfur dioxide is .0001 db and the smallest change detectable is .01 db the change due to sulfur dioxide will not be detected.

As a result of the theoretical work done during this experiment and mentioned earlier it was finally concluded that Figure 14 was the correct representation of the sulfur dioxide spectrum in the atmosphere in the microwave region and, since this experiment was designed to detect a line like that found in Figures 11 or 13, work on this experiment was stopped.

The fact that sulfur dioxide can not be detected by the previously described experiment has a broad application. In fact this result can be applied to any cavity frequency meter experiment. Although this experiment was unsuccessful because of the low power levels involved, the power absorbed by the sulfur dioxide could, in theory, be detected by increasing the pathlength between transmitter

and receiver, by transmitting more power, by using highly directive antennas, or by operating at a different absorption frequency in the microwave spectrum. While these parameters are alterable by the experimentalist and could be altered so that more power will be absorbed by the sulfur dioxide, the shape of the spectrum is not alterable since it is a fact of nature.

Since the success of the cavity frequency meter measurement technique depends not only on the power absorbed by the sulfur dioxide but also on the high resolution of the spectrum, the theoretical results (Figure 14) indicate the resolution of the spectrum is very low and thus any type of cavity frequency meter experiment would yield the same results.

CONCLUSION CONCERNING RECOMMENDATIONS FOR FUTURE STUDY IN THE INFRARED REGION

Based on the above work, a conclusion has been reached that the microwave spectrum is not at present feasible for use in remote detection of sulfur dioxide. As a result of this conclusion, a survey has been made of other areas of the spectrum with the possibility that they could prove useful for pollution study.

The first area surveyed was the ultra-violet region of the spectrum ranging from .25 to .40 μ . Chief researcher in this area has been Barringer (1970). Some Barringer equipment was used during the summer of 1971 by a research team at The University of Arizona to determine levels of sulfur dioxide pollution. Quantitative data were not available from this study at the time of this report since calibration cells were not available from Barringer Research. In detecting pollutant gases in the ultra-violet, the sun is used as a source, and the pollutant gases will absorb sunlight at certain discrete frequencies. Although this method is straightforward in theory, it appears to have a few major drawbacks. Most obvious is that no pollution data can be taken at night. In addition, because the sun is the source, pollution paths must always be slant paths through the upper atmosphere. To interpret

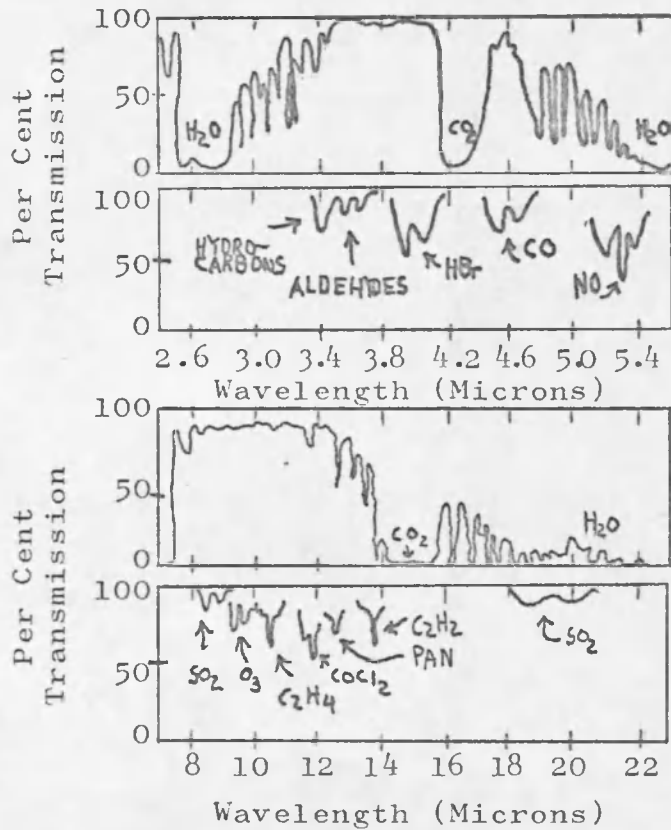
the pollution data correctly, information about meteorological conditions must also be taken at the same time so that the distribution of the pollutant in the air can be calculated. This requirement adds to the data that must be taken and also brings in new variables that must be dealt with in determining a pollution level in the ultra-violet. The ultra-violet is also limited in that not all gases have a resolvable signature in this region. The main gases that can be resolved at present are ozone, sulfur dioxide, and nitrogen dioxide. At the present time much study is being done to determine the effect of atmospheric scattering on the interpretation of the data taken in the ultra-violet region. Ludwig, Bartle, and Griggs (1968) have raised the question of whether or not the ultra-violet can give dependable quantitative data because of the effect of atmospheric scatterers and the difficulty in allowing for these effects. As a result of the above points, the ultra-violet does not seem promising.

Two other areas of the electromagnetic spectrum equally unpromising are the visible spectrum (.4 to .7 μ) and the far infrared (25 to 500 μ). The visible spectrum is not considered useful since almost no gases have absorption spectrum in this region. The far infrared is eliminated because, although rotational lines of many molecules exist in this region, the entire region is

blanketed by very strong atmospheric water vapor lines which prohibit detection of pollutants.

The remaining two regions of the spectrum to be considered for pollution studies are the regions from .7 to 2.5 μ (the near infrared) and 2.5 to 25 μ (the middle infrared). Unlike the other regions, both the near infrared and the middle infrared appear promising for pollution studies for the following reasons. The existence of infrared lasers has made the use of the sun as a source unnecessary. In addition, the laser permits pollution data to be taken along horizontal paths and eliminates the need for meteorological data needed when the sun is used as a source and the absorption paths are slant paths through the atmosphere. Another advantage of using a laser as a source instead of the sun is that the pollution data can be taken at night. Moreover, almost all gases contain an absorption signature in these regions. Figure 26 (Hanst, 1970) shows some of the pollutants found in the middle infrared region. Because of the existence of "windows" in these regions water vapor blanking also does not present a problem. An example of some of the common "windows" in the middle infrared is also shown in Figure 26.

Although either of the two above mentioned regions would in theory work well for pollution studies, properties of the pollutants themselves have made the middle infrared a more promising region than the near infrared. The



Path Length ~ 1000 ft
 Random Air Sample at
 Atmospheric Pressure
 SO₂ ~ .03 ppm
 CO ~ 2 ppm
 NO ~ .5 ppm
 C₂H₂ ~ not available
 O₃ ~ .05 ppm
 C₂H₄ ~ .02 ppm
 PAN ~ .05 ppm

Figure 26. Middle Infrared Spectrum

advantage of the middle infrared over the near infrared results because the pollutant molecules have fundamental and higher harmonic vibrational lines. The higher harmonic lines of a pollutant gas are many times weaker than the fundamental lines, and these harmonic lines usually fall in the near infrared region. Thus, for ease of detection, the fundamental vibrational lines will absorb infrared radiation much more strongly than the corresponding harmonic of the same line measured in the near infrared. In this way trace amounts of pollutants can be measured in the middle infrared where they would be too faint to detect in the near infrared.

Recently at the Lincoln Laboratory in Lexington Massachusetts, researchers under E. D. Hinkley (Hinkley and Kelly, 1971) have developed a tunable laser for the 8.6μ window of the middle infrared. Figure 27 (Shelton, Nielsen, and Fletcher, 1953) shows a theoretical picture of the vibration-rotation fine structure of the sulfur dioxide molecule found at this wavelength. In addition, a recent paper by Hanst and Morreal (1968) suggests a method whereby this pollutant could be measured. In this method two lasers would be used; one would be locked on a sulfur dioxide vibration-rotation line, and another would be locked off the line. The difference between the amplitudes of the two lines could then be continually monitored.

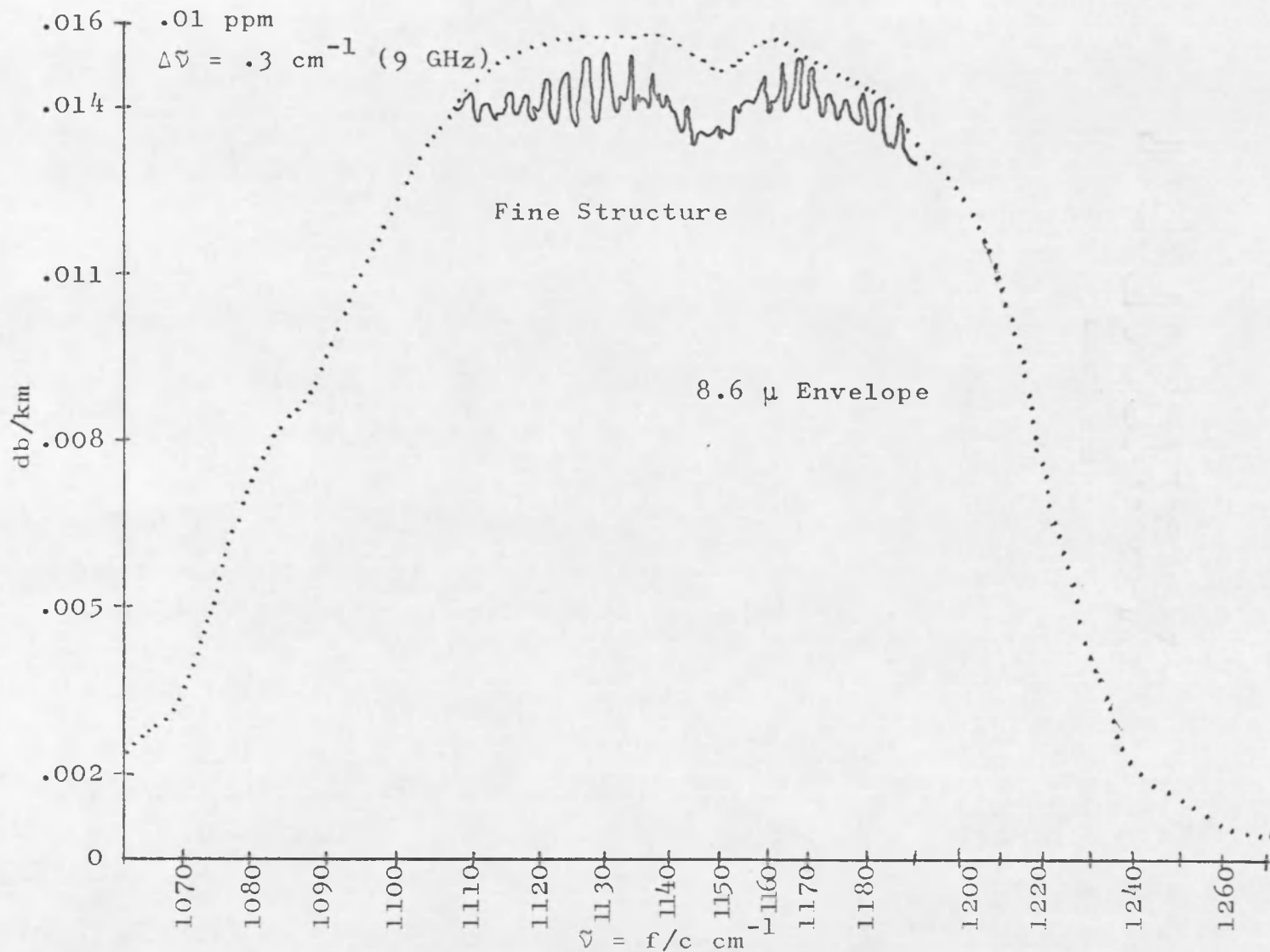


Figure 27. 8.6 μ Spectrum of SO_2

At the date of this paper (fall 1971), no field testing work in the middle infrared over long atmospheric paths has been reported. In addition, it appears that only three places in the country are at present active in this field: General Electric Corporation in Syracuse New York under Dr. Larry Snowman, Tulane University under Dr. Edward Christy, and the previously mentioned Lincoln Laboratory under Dr. E. D. Hinkley. From the state of the art at the present time, it would seem that there is room for applied research in this area.

LIST OF SYMBOLS

English letters

A	area
A,B,C	quantum mechanical proportionality constant
E	energy
f	fractional molecular density
F	force, free space loss
G	antenna gain
h	Planck's constant
I	moment of inertia
J	time average power flow
j	photon flux
J,K,M	quantum numbers
k	Boltzman's constant
l	distance
m	mass
MDS	minimum detectable signal
M	signal level margin
N,N	molecular density
P	power, transition probability, pressure
q	charge
R,r	radial distance
S	power density
T	temperature
t	time
V	volume
W	energy

Greek letters

α	absorption coefficient
Δ	small change
$\Delta\nu$	line width parameter
ϵ_0	free space dielectric constant
λ	modifying factor of the dipole moment matrix
κ	Ray's asymmetry parameter
μ	dipole moment matrix, mass
ν	frequency
ν_0	resonant frequency
τ	torque
Ψ	quantum mechanical wave function
ω	speed of rotation

SELECTED BIBLIOGRAPHY

- Angelakos, Diogenes, and Thomas Everhart. Microwave Communication. New York: McGraw-Hill, 1968.
- Barringer, A. R. Collection of papers on Correlation Spectroscopy, unpublished. Barringer Research Corp., Canada, 1970.
- Barrow, Gordon. Physical Chemistry. 2nd. ed. New York: McGraw-Hill, 1966.
- Beer, Ferdinand, and E. Russell Johnston, Jr. Vector Mechanics for Engineers, Statics and Dynamics. New York: McGraw-Hill, 1962.
- Bignell, K., F. Saiedy, and P. A. Sheppard. "On the Atmospheric Infrared Continuum," Journal of the Optical Society of America, LIII (April, 1963), 466-479.
- Bird, G. R., and C. H. Townes. "Sulfur Bonds and the Quadrupole Moments of O, S, and Se Isotopes," Physical Review, XCIV (June, 1954), 1203-1208.
- Bloor, D. "Bibliography of Far Infrared Spectroscopy," Infrared Physics, X (March, 1970), 1-55.
- Cleeton, C. E., and N. H. Williams. "Electromagnetic Waves of 1.1 cm Wave-length and the Absorption Spectrum of Ammonia," Physical Review, XLV (February 15, 1934), 234-237.
- Crable, George, and William V. Smith. "The Structure and Dipole Moment of SO₂ from Microwave Spectra," The Journal of Chemical Physics, XIX (April, 1951), 502.
- Cross, Paul, R. M. Hainer, Gilbert W. King, and Arthur D. Little. "The Asymmetric Rotor II," The Journal of Chemical Physics, XII (June, 1944), 210-243.
- Dailey, B. P., and E. B. Wilson. "Microwave Spectra of Several Polyatomic Molecules," Physical Review, LXXII (1947), 522.

- Dailey, B. P., S. Golden, and E. Bright Wilson, Jr. "Preliminary Analysis of the Microwave Spectrum of SO_2 ," Physical Review, LXXII (1947), 871-872.
- Feynman, Richard, Robert B. Leighton, and Mathew Sands. The Feynman Lectures on Physics. 3 volumes. Reading, Mass.: Addison-Wesley, 1963.
- Ghosh, S. N., and H. D. Edwards. "Rotational Frequencies and Absorption Coefficients of Atmospheric Gases," Air Force Surveys in Geophysics, Report 82 (March, 1956).
- Gordy, Walter, William V. Smith, and Ralph F. Trambarulo. Microwave Spectroscopy. New York: John Wiley and Sons, 1953.
- Hanst, Philip L. "Infrared Spectroscopy and Infrared Lasers in Air Pollution Research and Monitoring," Applied Spectroscopy, XXIV, No. 2 (1970), 161-174.
- Hanst, Philip L., and John A. Morreal. "Detection and Measurement of Air Pollutants by Absorptions of Infrared Radiation," Journal of the Air Pollution Control Association, XVIII (November, 1968), 754-759.
- Heitler, W. The Quantum Theory of Radiation. 2nd ed. Oxford: Oxford University Press, 1944.
- Hershberger, W. D. "The Absorption of Microwaves by Gases," Journal of Applied Physics, XVII (June, 1946), 495-500.
- Hildebrand, Francis. Advanced Calculus for Applications. Englewood Cliffs, N. J.: Prentice-Hall, 1962.
- Hinkley, Ed, and P. L. Kelly. "Detection of Air Pollutants with Tunable Diode Lasers," Science, CLXXI (February 19, 1971), 635-639.
- Ingram, D. J. E. Spectroscopy at Radio and Microwave Frequencies. New York: Plenum Press, 1967.
- Johnson, Curtis. Field and Wave Electrodynamics. New York: McGraw-Hill, 1965.
- Karplus, Robert, and Julian Schwinger. "A Note on Saturation in Microwave Spectroscopy," Physical Review, LXXIII (May 1, 1948), 1020-1026.

- Kay, R. B. "Absorption Spectra Apparatus Using Optical Correlation for the Detection of Trace Amounts of SO_2 ," Applied Optics, VI (April, 1967), 776-778.
- King, Gilbert, Arthur D. Little, R. M. Hainer, and Paul C. Cross. "The Asymmetric Rotor I," Journal of Chemical Physics, XI (January, 1943), 27-42.
- Kivelson, Daniel. "The Determination of the Potential Constants of SO_2 from Centrifugal Distortion Effects," The Journal of Chemical Physics, XXII (May, 1954), 904-908.
- Kosow, Irving. Microwave Theory and Measurement. Englewood Cliffs, N. J.: Prentice-Hall, 1964.
- Leavitt, Mark K. Unpublished manuscript, The University of Arizona, 1971.
- Ludwig, C. B., R. Bartle, and M. Griggs. "Study of Air Pollutant Detection by Remote Sensors," NASA Contractors Report CR 1380, Convair Division, General Dynamics Corp., December, 1968.
- Mahan, Bruce. University Chemistry. Reading, Mass.: Addison-Wesley, 1965.
- Mees, Quentin, principal investigator. Tucson Air Pollution, 1959-1964. Tucson: College of Engineering, University of Arizona, 1964.
- Meierdierks, John. Personal communication, Varian Associates, 1970.
- Pauling, Linus, and E. B. Wilson. Introduction to Quantum Mechanics. New York: McGraw-Hill, 1935.
- Pierson, Raymond H., Aaron N. Fletcher, and E. St. Clair Gantz. "Catalog of Infrared Spectra for Qualitative Analysis of Gases," Analytical Chemistry, XXVIII (August, 1956), 1218-1239.
- Quintenz, Jeff. Unpublished manuscript, The University of Arizona, 1971.
- Roche, J. F., Herman Lake, Donald T. Worthington, Carson Kl. Tsao, and Joseph T. de Bettencourt. "Radio Propagation at 27-40 GHz," IEEE Transactions on Antennas and Propagation, AP-18 (July, 1970), 452-563.

- Sadler Standard Spectra Tables. Philadelphia: Sadler Research Laboratories, 1967.
- Sears, Francis W., and Mark Zemansky. University Physics. 2nd ed. Reading, Mass.: Addison-Wesley, 1955.
- Shelton, R. D., A. H. Nielsen, and W. H. Fletcher. "The Infrared Spectrum and Molecular Constants of Sulfur Dioxide," Journal of Chemical Physics, XXI (December, 1953), 2178-2183.
- Silver, Samuel. Microwave Antenna Theory and Design. New York: Dover Publications, 1965.
- Sirvetz, M. H. "The Microwave Spectrum of Sulfur Dioxide," Journal of Chemical Physics, XIX (July, 1951), 938-941.
- "Solid State Lasers Beam in on Air Pollution," New Scientist and Science Journal (March 4, 1947), p. 489.
- Sproull, Robert. Modern Physics. 2nd ed. New York: John Wiley and Sons, 1965.
- Sugden, T. M., and C. N. Kenney. Microwave Spectroscopy of Gases. London: D. Van Nostrand Co., 1965.
- Symon, Keith. Mechanics. 2nd ed. Reading, Mass.: Addison-Wesley, 1960.
- Townes, C. H. Personal communication, University of California, Berkeley, 1971.
- Townes, C. H., and A. L. Schawlow. Microwave Spectroscopy. New York: McGraw-Hill, 1955.
- Valley, S. L., ed. Handbook of Geophysics and Space Environments. New York: McGraw-Hill, 1965.
- Van Vleck, J. H., and Henry Margenau. "Collision Theories of Pressure Broadening of Spectral Lines," Physical Review, LXXVI (October 15, 1949), 1211-1214.
- Van Vleck, J. H., and V. F. Weisskopf. "On the Shape of Collision-Broadening Lines," Review of Modern Physics, XVII (April-July, 1945), 227-236.
- Walter, John E., and W. D. Hershberger. "Absorption of Microwaves by Gases. II," Journal of Applied Physics, XVII (October, 1946), 814-822.

Westman, H. P., ed. Reference Data for Radio Engineers.
4th ed. New York: International Telephone and
Telegraph, 1956.

Wichmann, Eyvind. Quantum Physics. Vol. 4. New York:
McGraw-Hill, 1971.

